Modeling and Simulation of Surface Roughness in Improved Magnetorheological Honing Process

A Dissertation Submitted

In partial fulfillment of requirement for the award of the degree of

Master of Engineering

in

CAD/CAM Engineering

by

Sunil Kumar Paswan

Roll No.: 801481023

Under the Supervision of

Dr. Anant Kumar Singh

Assistant Professor

DEPARTMENT OF MECHANICAL ENGINEERING

THAPAR UNIVERSITY

PATIALA-147004, INDIA

July, 2016

CERTIFICATE

I hereby declare that work done in this thesis entitled, **"Modeling and Simulation of Surface Roughness in Improved Magnetorheological Honing Process"** is authentic record of my own work carried out in completing the thesis requirement for the degree of **Master of Engineering in CAD/CAM Engineering** at Thapar University, Patiala, under the guidance of "**Dr. Anant Kumar Singh**", Assistant Professor, Mechanical Engineering Department, Thapar University, Patiala

This matter embodied in this report has not been submitted in part or full to any other university or institute for the award of any degree.

Date: 29/07/2016

Sunil Kumar Paswan
(801481023)

This is to certify that above statement made by the student concerned is correct to the best of our knowledge and belief.

Dr. Anant Kumar Singh
Assistant Professor
Department of Mechanical Engineering
Thapar University, Patiala-147004

Countersigned by:

Dr. S.K. Mohapatra
Senior Professor and Head
Mechanical Engineering Department
Thapar University, Patiala-147004

Dr. S.S. Bhatia
Dean of Academic Affairs
Thapar University, Patiala-147004

ii

Dedicated to

My mother Late Sumitra Devi

Acknowledgement

I am truly and deeply thankful to my mentor, **Dr. Anant Kumar Singh** for the amount of knowledge that he shared with me, along with the countless amounts of time that he spent for me. The enthusiasm and effort that he had put into this topic and to make me better off will always be remembered. I heartily thank him, for offering me this wonderful opportunity. Without his guidance and persistent help, this thesis would not have been possible. For all his help and guidance throughout the years, I am indebted to him.

I thank the entire faculty and staff of Mechanical Engineering Department, Thapar University, for their help and moral support.

I also acknowledges the use of facilities of Metrology Lab of Mechanical Engineering Department, Thapar University, Patiala, for experimentation part of my dissertation.

Sunil Kumar Paswan

Abstract

A novel improved magnetorheological honing process is developed for finishing of internal geometries of ferromagnetic cylindrical workpiece as existing magnetorheological fluid based finishing processes are not found suitable to finish the internal surface of cylindrical ferromagnetic components. The performance of finishing action to enhance material removal in the developed process mainly depends on the normal force acting on abrasive particles due to magnetic behavior of the carbonyl iron particles with magnetic field in magnetorheological polishing fluid. Also, it depends on the shear force acting on surface by abrasive particles due to translational and rotational motion of tool as likely similar to the honing operation. In the present work, modeling of magnetic field induced in magnetorheological finishing fluid and the surface roughness values with the effect of finishing cycles have been done. To validate the model and understand the material removal mechanism during finishing in improved magnetorheological honing process, the experiments have been performed on the internal surface of cylindrical ferromagnetic workpiece with the three different sets of finishing cycles. The surface roughness of cylindrical workpiece has experimentally measured with Mitutoyo SJ-400 surftest and to understand material removal mechanism during finishing of the workpiece surface, the scanning electron microscopy has been also performed. The theoretical induced magnetic field in magnetorheological finishing fluid and surface roughness with number of finishing cycles were calculated. The calculated values were validated with experimentally for the same number of finishing cycles and conditions. The theoretical calculated surface roughness values with the number of finishing cycles have been compared with the experimental obtained surface roughness values. Both were found in close agreement within 4.54 %. Thus, the present improved magnetorheological finishing process is found suitable for finishing of internal surface of cylindrical ferromagnetic components which leads to the functional applications of cylindrical ferromagnetic components as compared to traditional finishing techniques.

Keywords: Magnetorheological honing process, MRP fluid, cylindrical workpiece

Contents

List of Figures

List of Tables

Nomenclature

A	area of MRP fluid layer (mm^2)
V_{MRPF}	volume of MRP fluid (mm^3)
V_{CIP}	volume of carbonyl iron particle (mm^3)
F_m	force due to magnetic field (N)
D_g	diameter of abrasive grains (mm)
H_{BHN}	brinell hardness number (BHN)
χ_m	mass of magnetic susceptibility (kg/m^3)
μ_0	magnetic permeability of space (N/A^2)
d	depth of indentation (mm)
V_{single_CIP}	volume of single CIP (mm^3)
H	magnetic field strength (A/m)
B	magnetic field density (T)
R_a	centerline average roughness value (µm)
F_{normal}	normal force (N)
F_{Ts}	Tangential shear force (N)
D_i	diameter of indentation (mm)
N_g	number of active grain per cycle
m	mass of a single CIP particle (kg)
μ_r	relative permeability (N/A^2)
F_t	Tangential force (N)
F_{Ls}	Longitudinal shear force (N)

Chapter 1 Introduction

In recent years, the precision finishing technologies have developed with tremendous rate which has immense effect on the development of new product and material [1]. Due to accession of these new material and complicated product in shape, geometry and size, manufacturing personals are meeting to challenge of finishing and machining to fulfill the functional requirement. Traditional finishing processes are those processes whose finishing tools lack of flexibility during finishing the workpiece of complex geometry, harder material and shape variation [2]. Some examples of these finishing processes are grinding, honing, lapping etc. [1]. To overcome these limitations researchers have developed non-traditional finishing processes. These non-traditional processes have so many common traits, like these processes can utilize flexible abrading medium for finishing and are capable to finish complex geometrical workpiece surfaces. The flexible abrading medium are prepared by mixing the constituents material (abrasives) in the base medium like air or liquid [3]. For finishing operation some of these processes use magnetically influenced smart fluid such as magnetorheological polishing fluid as abrasives carrier [3]. The processes which use such type of smart fluids are magnetic fluid grinding [2], magnetorheological finishing [3], magneto-abrasive flow machining [4], and magnetorheological abrasive flow finishing [5]. Magnetorheological polishing (MRP) fluid based honing process is such type of finishing process which uses MRP fluid as abrasive carrier for finishing action and simultaneous rotary and translational motion to perform finishing action effectively [1]. Magnetorheological finishing (MRF) is a potent process for finishing complex shape of optical object with accuracy up to 50 nm and surface roughness value less than 1 nm [6]. First time Magnetorheological finishing was developed by the Luikov Institute of Heat and Mass Transfer in Minsk in 1980 by the leadership of William Kordonski [3]. Magnetorheological polishing (MRP) fluids are composed of in fixed proportion of carbonyl iron particle (CIP), non-magnetic SiC abrasive particle of mess size 800, and base liquid like natural oil, mineral oil, water, glycol or grease AP3 [5].

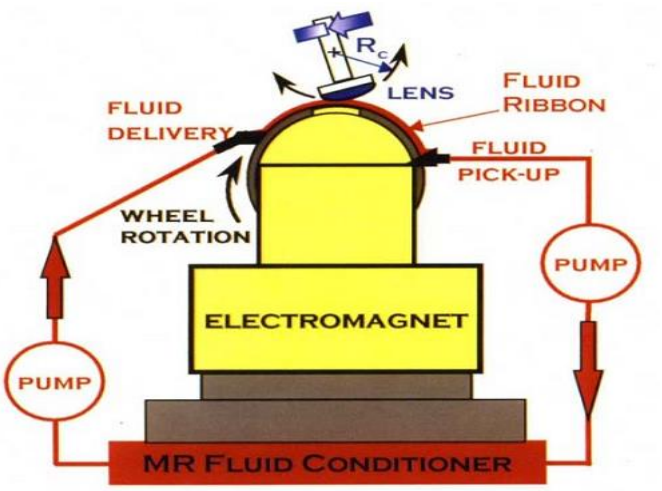

Figure 1.1: MRF process setup [1]

A part produced by any manufacturing process like casting, forging, forming or machining, is necessarily finished for finalize the operation. Sometimes this finishing operation takes take 10-15% cost of total manufacturing cost of the product [3]. These processes are selected as appropriate finishing processes for particular product due to its capability of minimizing the cost, time and maximizing the surface quality of product [4]. This paper deals about surface improvement which can be done by finishing operation. Finishing processes have been divided into two broad class [6].

- Traditional finishing processes: This category of finishing processes includes grinding, honing, lapping, and super finishing.
- Advanced finishing processes: this category of finishing process includes abrasive flow machining (AFM), magnetorheological finishing (MRF), magnetorheological abrasive flow finishing (MRAFF), elastic emission machining (EEM), chemo mechanical polishing (CMP) and magnetic float polishing (MFP).

1.1 Traditional Finishing Processes

In traditional finishing processes, the finishing tool and workpiece always remain in direct contact, during finishing operation due to their relative motion against each other friction is caused and significant tool wearing takes place [6]. Some important examples of this broad group of finishing process are, grinding, lapping, honing, etc. Material removal rate of these processes depends on the mechanical properties of the workpiece [5]. In most of the traditional finishing processes relative motions between tool and workpiece are either rotary or circulating

therefore, these are limited to finish the workpiece of flat geometry or cylindrical and for small cavities, slits, blind or through holes these process are found difficult to apply [7].

1.1.1 Grinding

In this process, the protuberant active grains removes the layer of material of thickness up to 1 mm which results to finish action on workpiece. Therefore, grinding is a surface finishing process in which convex abrasive particles are confined in a joined grinding wheel that operates at high speed [6]. The grinding wheel is of disc shape and is suitable for high rotational speeds. Material removal mechanism in grinding process is as shown in figure 1.2. The dressing up and truing is the non-productive activity while finishing operation taking place. Therefore, to enhance the finishing capability electrolytic in-process dressing (ELID) [8] is applied, in which dressing of the grinding wheel is done during the process as shown in figure 1.3.

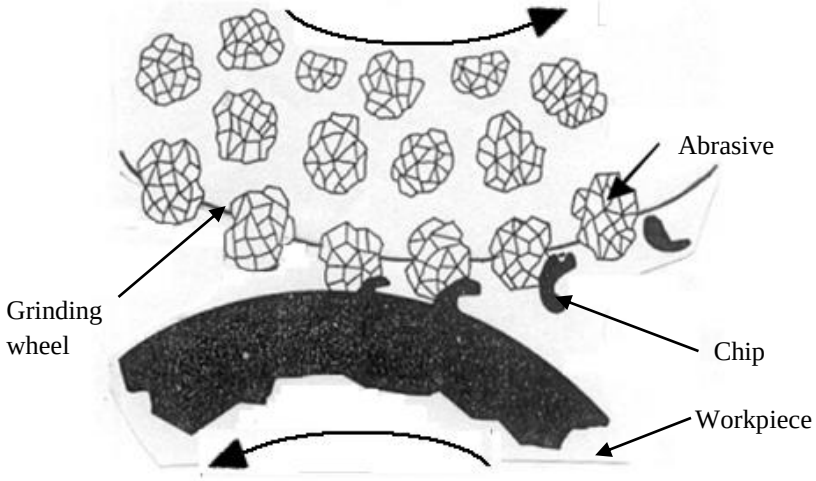

Figure 1.2: Grinding operation [8]

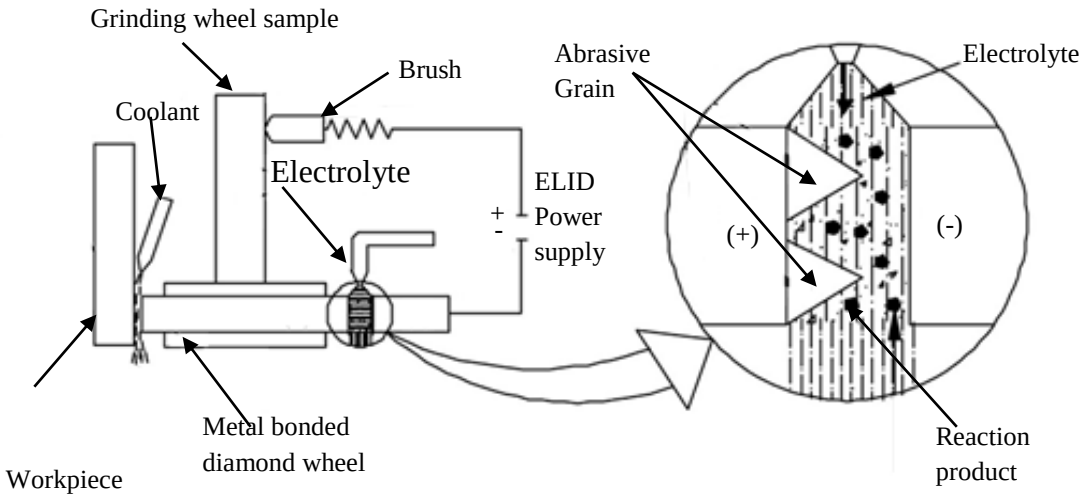

Figure 1.3: Electrolytic-in-process dressing (ELID) [8]

1.1.2 Honing

Honing is a material removal mechanism for cylindrical workpiece performed by the tool which is able to perform simultaneous motions rotational and translation. The honing tool has abrasive sticks in form of set of the sticks in number three to a dozen. The sticks are maintained at equal space around the border of the tool [6]. They are seized to workpiece surface with activation precised minimal pressure, mostly small springs are used. The tool is given simultaneously rotational and reciprocation motion, which produces a crosshatched lay pattern of lower surface roughness as shown in figure 1.4 [7, 8].

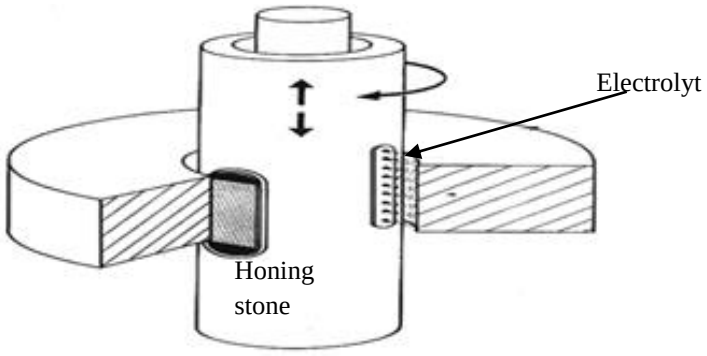

Figure 1.4: Electrolytic honing process [8]

1.1.3 Lapping

Lapping is a finishing process which uses unfastened abrasives to finish the surface. This process is based on three body abrasive wear principle. In this process finishing action take place through graze by abrasive particles lying in between peaks and valleys of workpiece

surface [7]. With introduction of abrasive particles in between space of lap and workpiece, on moving lap relative to workpiece surface in arbitrary direction and with certain pressure abrasion takes place as shown in figure 1.5. This process is employed to finish the component of curved shape and three dimensional shape by designing of lap as per requirement. Amount material removal in this process is insignificant because this is used for improvement of surfaces quality and accuracy.

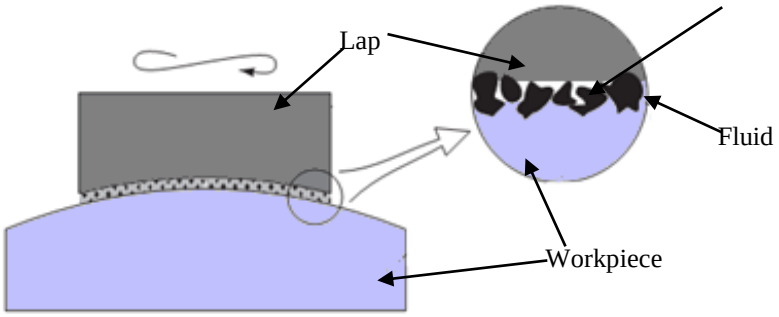

Figure 1.5: Lap in lapping process and finishing action of suspended abrasive particles [7]

1.1.4 Super Finishing

Super finishing is a material removal mechanism similar to the honing process, but difference is of using a single abrasive stick in place of multiple unlike in honing as it can be seen in figure 1.6. During oscillating motion of the abrasive stick higher frequency and smaller amplitudes are maintained [7]. In this process size of abrasives and pressure used on abrasive stick are smaller and to cool the workpiece cutting fluid is used, it also wash away the chips.

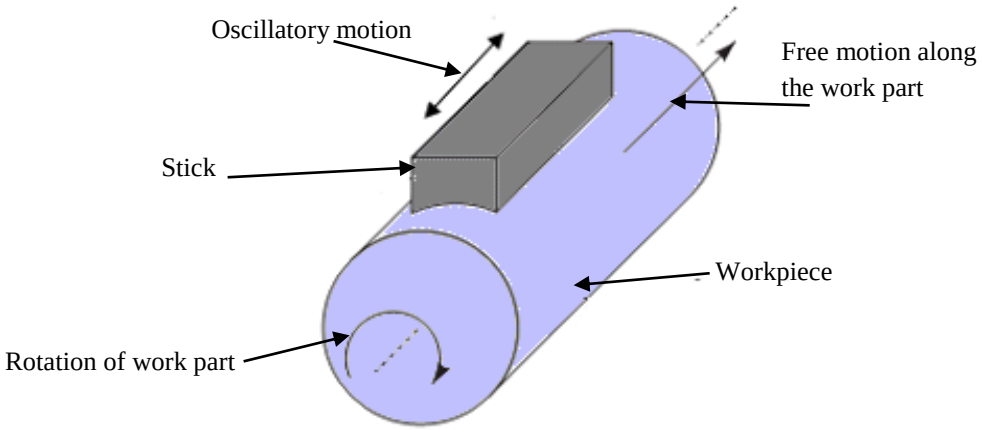

Figure 1.6: Super finishing process [7]

1.2 Advanced Finishing Processes

Inventions of large number of materials ranging softer to harder, which have led to the situation of difficult to machine against their high strength, temperature resistant, hardness etc. characteristics to get extra ordinary surface quality. Smart material and Nano-materials are the demand of current industries. To make the product of harder material of complex geometry and of flexible size traditional processes found incapable [4]. Therefore, to remove bulk material, for high precision in surface, to improve quality control, to advance flexibility in changeability of components, and strengthening the component be reducing wear and fatigue advanced finishing processes are developed [3]. All of the advanced finishing processes are further divided into two categories [6].

- Without external control of force
- With external control of force

1.2.1 Advanced Finishing Processes without Control of External Force

These type of finishing processes are used to ultrafine finishing the workpiece surface but the force acting during finishing on the abrasive particle can't be control with external force. Some examples of this type are: abrasive flow machining (AFM), chemo mechanical polishing (CMP) and elastic emission machining (EEM) [6].

1.2.1.1 Abrasive Flow Machining (AFM)

Abrasive Flow Machining (AFM) is one of the prominent type of advanced finishing process. It was initially known in the era of 1960s as a technique to polish the surface, deburr the workpiece surface and finish the surface where difficult to reach by flowing abrasive loaded viscoelastic polymer [8]. This process was found as a technique for deburring and finishing hydraulic and fuel system components of aircraft in aerospace industries [7]. Due to the flow ability of abrasive laden fluid AFM process can polish all type of workpiece with intricate and complex geometry of shape [8]. The process setup and mechanism of process can be seen as in figure 1.7.

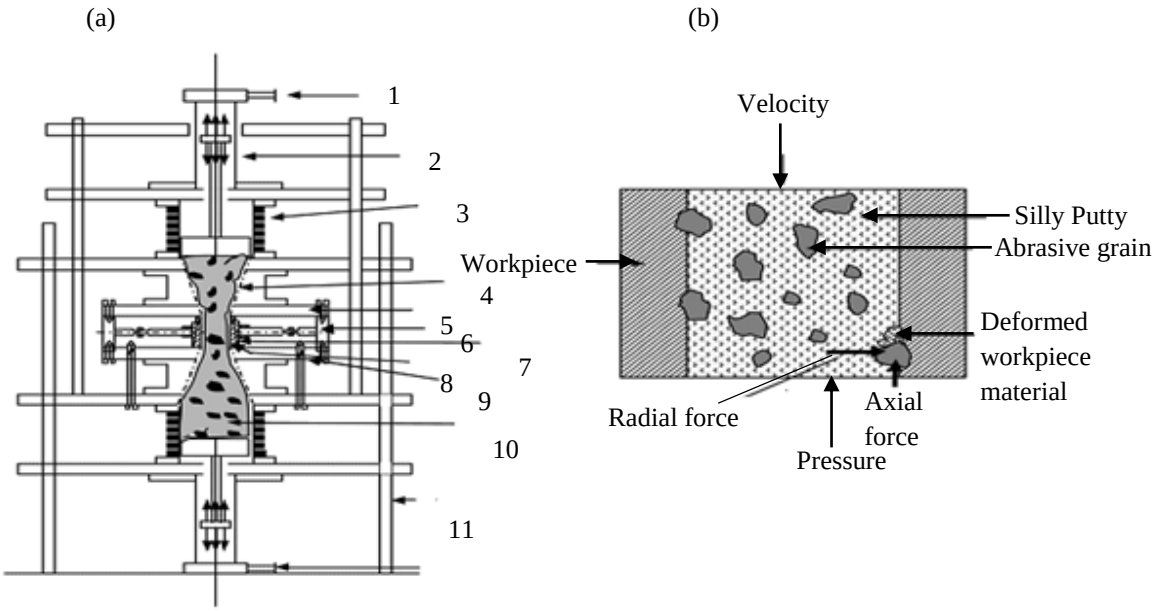

Figure 1.7: (a) Illustrative drawing of experimental setup: 1-Hydraulic oil inlet, 2-Hydraulic cylinder, 3-Medium cylinder, 4-Smooth entry profile, 5-Top cover plate, 6-Dynamometer, 7-Central hub, 8-Split cylindrical fixture with workpiece, 9-Bottom cover plate, 10-Support frame, 11-Hydraulic oil outlet, 12-Medium with abrasive particles and (b) Forces acting on grain [8]

1.2.1.2 Chemo-Mechanical Polishing (CMP)

Chemo-Mechanical polishing (CMP) is a material removal mechanism which is used in the semiconductor manufacturing industries. During the process, combined action of mechanical and chemical take place to perform the operation [8]. Chemical reaction between silica slurry and the workpiece take place as a chemical part of this process and the product of reaction is removed as mechanical action of this process [6]. Therefore, the finishing action in this process is performed as shown in figure 1.8.

Figure 1.8: Chemo-Mechanical Process [6]

1.2.1. 3 Elastic Emission Machining (EEM)

This mechanism is used to get the surface finish quality up to atomic level through mechanical action [9]. It has potential to give completely mirrored surface without any crystallographic and physical disturbed in work surface [9]. Methodology of this process is striking tiny abrasive particles to the group of atoms or individual atom and detaches them from surface of workpiece. Finishing action in this process is associated with surface energy phenomenon in which each abrasive particles eradicates atoms on contacting the workpiece surface [9]. The process can be understood better from the figure 1.9.

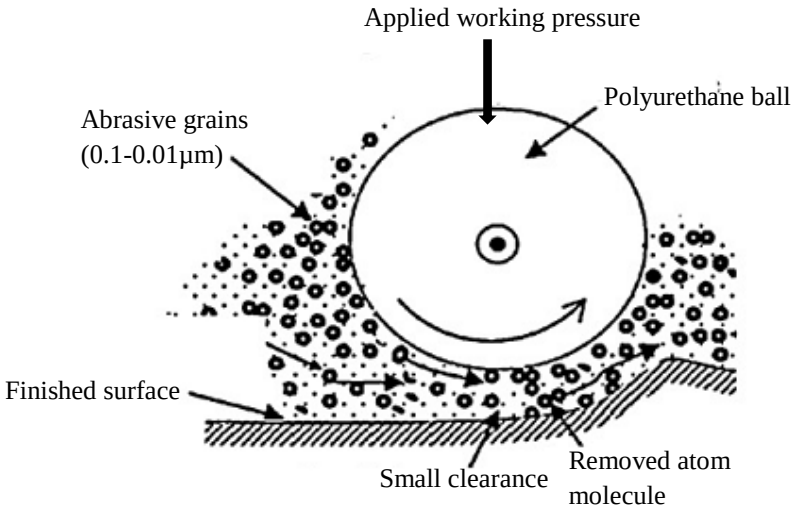

Figure 1.9: Elastic Emission Machining (EEM) [6]

1.2.2 Advanced Finishing Processes with External Control of Force

Advanced finishing processes without external control of force category of finishing process includes MAF, MRF, MRAFF, MFP, BEMRF, and MRAH. In these processes, the forces inducing on abrasive particles are regulated externally by varying the dependent parameter of the finishing action like magnetic field density, working gap, different proportions of abrasives, magnetic particles, base medium etc. [6].

1.2.2.1 Magnetorheological Finishing (MRF)

In most of the cases material used for making the highly precised lenses are generally inelastic material such as glass which has great possibility of crack while finishing action taking place. Therefore, to get rid of such type of difficulties in abrasion of lenses, Centre for Optics Manufacturing (COM) at Rochester N.Y. has introduced a technique to finish the lens through

automation, is known as Magnetorheological Finishing (MRF) [3]. This process depends on the rheological behavior of a smart fluid i.e. magnetorheological (MR) fluid. An ideal MR fluid shows Newtonian behavior in absence of magnetic field density and as the magnetic field activated magnetizable particles get stiffen and by rubbing on workpiece finishing action take place. This process setup is shown as in figure 1.1.

1.2.2.2 Magnetorheological Abrasive Flow Finishing (MRAFF)

To resume the versatility of abrasive flow machining process and to add some extra feature like absolutist and controllability in rheological behavior of MRP fluid, a new hybridized finishing process has been developed known as Magnetorheological abrasive flow finishing (MRAFF) process [5]. MRP fluid used in this possess rheological behavior which can be controlled by external magnetic field. This process has potential to finish complicated internal and external geometries up to the surface roughness values in nano meter [2]. The performance of this process depends on the magnetic effect shown by carbonyl iron particles of MRP fluid, number of finishing cycles, and exile pressure [10]. Mechanism of the MRAFF process is as shown in the figure 1.10.

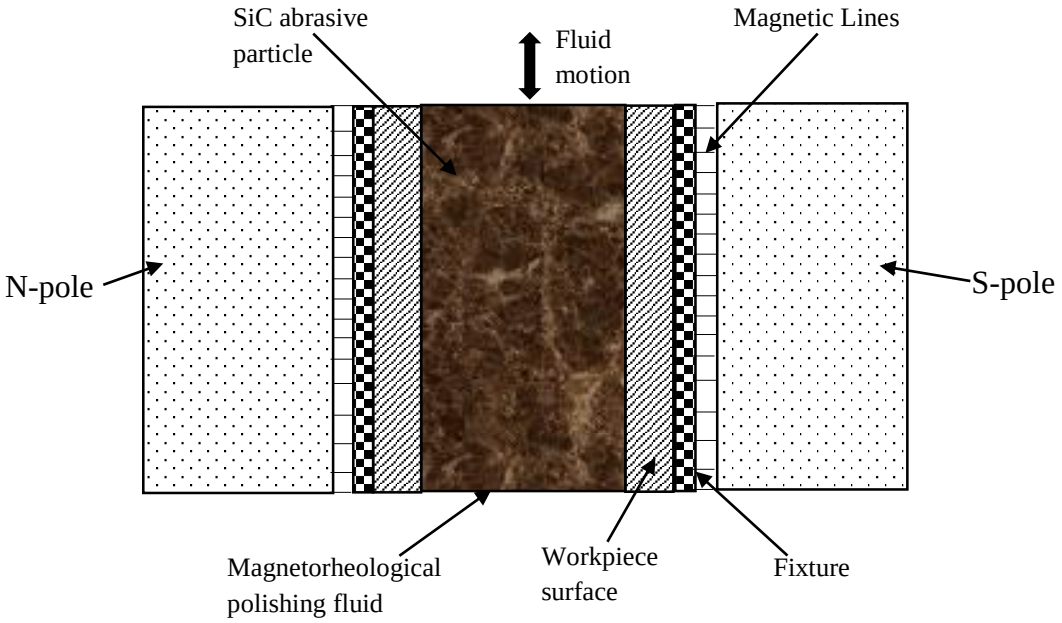

Figure 1.10: Mechanism of MRAFF action [10]

1.2.2.3 Magnetic Float Polishing (MFP)

Almost all the finishing processes present, have been developed to finish flat, cylindrical or combination of these two types of geometry, which approaching to complex three dimensional

surface. To finish sphere-shaped surfaces is parallel important but none of the available finishing process is able to finish spherical surfaces. Therefore, to finish spherical surface the Magnetic Float Polishing (MFP) [11] process has been developed. In this process magnetic field is used to backing abrasive slurry during abrasion. This process uses ferro-hydrodynamic properties of polishing fluid that ascends a non-magnetic float and abrasive particles suspended on application of magnet field to finish the workpiece surface.

1.2.2. 4 Magnetic Abrasive Finishing (MAF)

To finish the workpiece of flat sized and made up of hard to machine material up to nano level, the earlier discussed finishing processes are found unqualified. Therefore, Magnetic abrasive finishing (MAF) process is introduced for effective and exact finishing of workpieces to get required surface quality [12]. This process uses ferromagnetic abrasive particles as abrasive, made up of sintered ferromagnetic particles and tiny abrasive particles, such as Al2O3, SiC, CBN or diamond [8]. This process is also used to remove film of thin oxide from rotating shaft at high speed and for polishing the shaft [13]. It has been employed to finish exterior and interior surfaces of cylindrical workpiece, vacuum tubes etc., and the surfaces are finished efficiently as well as precisely due to the capable to control the mutual motion abrasive particles and workpiece surface as shown in figure 1.11. [14].

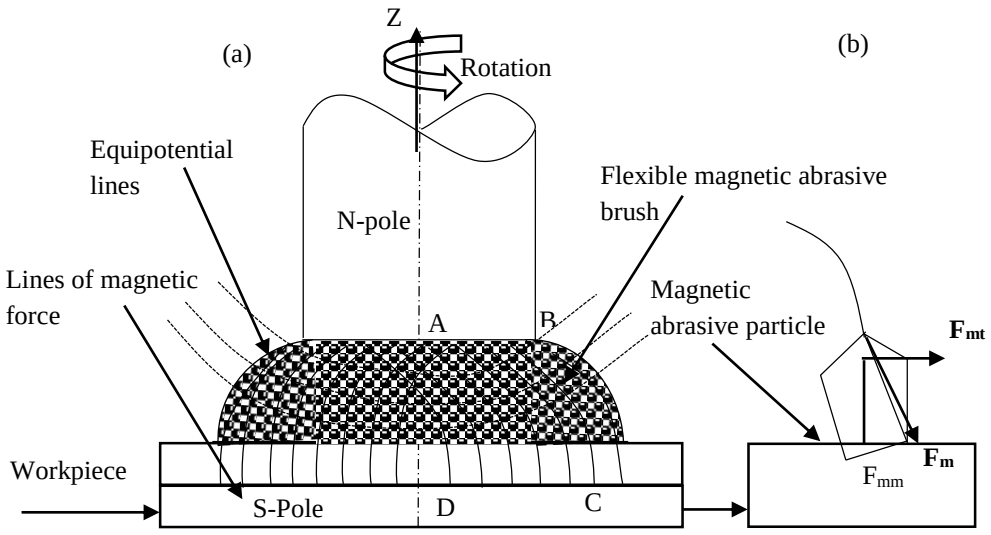

Fig. 1.11: (a) Flat magnetic abrasive finishing, (b) Magnified view of finishing area, workpiece and electromagnetic coil [13]

1.2.2. 5 Ball End Magnetorheological Finishing (BRMRF) Process

Ball end magnetorheological finishing (BEMRF) process is employed to finish flat and three dimensional workpiece surface using MRP fluid. In this process pressurized MRP fluid is allowed to flow through the Centre of core. As MRP fluid comes in between the gap of core and workpiece due to induced magnetic field at any position in gap the MRP fluid gets stiffened. The stiffened MRP fluid forms shape of ball end on the tip of the tool. Therefore, by providing rotational motion to the tool it finishes the workpiece surface of required level by adjusting relying parameters [15]. The setup of BEMRF is shown in figure 1.12.

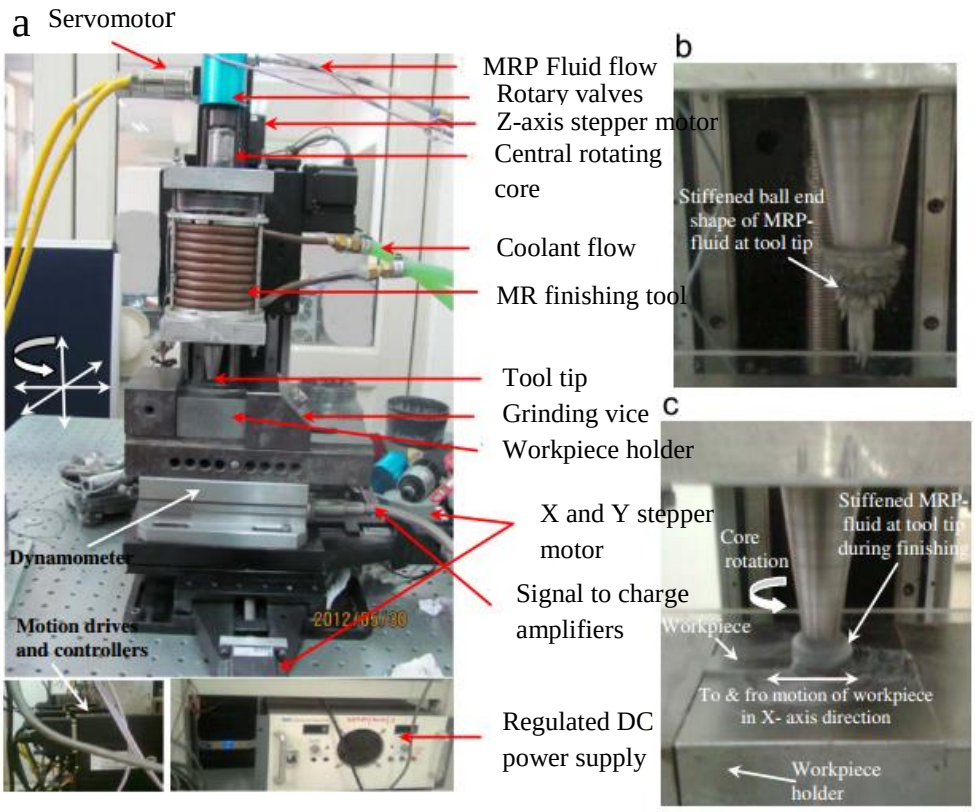

Figure 1.12: Picture of BEMRF experimentation setup for (a) measurement of induced magnetic field, normal force and rheological behavior of MRP fluid, (b) tip surface of tool as electromagnet was switched ON and (c) during surface finishing by abrasion action [15]

1.2.2. 6 Magnetorheological Abrasive Honing (MRAH) Process

Magnetorheological abrasive honing (MRAH) process is type advanced finishing process which is used to finish external surface of cylindrical objects [7]. In this scheme cylindrical object is attached with spindle and allowed to rotate and perform up and down motion simultaneously in MRP fluid as shown in fig.1.13. Magnetic field caused by electromagnet coil

aligns and stiffens the CIP particles [15]. The active abrasive particles [8], during the simultaneous rotational and translational motion indent into surface and remove the material in chips form. Magnetic normal force is liable for indentation of abrasive particle into workpiece surface and due to rotational and translational motion material removal in chips form takes place [16].

1.3 Advantages of using MR fluid Based Finishing Processes over Traditional and Without External Force Controlled Advanced Finishing Process.

Advantages of using MR fluid based finishing processes over tarditional and without external force comtrolled finishing processes are as follows

- Capability to finish up to nanometer of centerline average roughness value.
- Capability to finish hard material, ferromagnetic as well as non-magnetic material.
- Capable to precised control therefore, it results to accurate and fine finishing.
- There is no fear of damage caused by heat, grains deformation and stress residual.
- There is no wear of cutting tool can take place because of continuous replacement of abrasive particle.

1.4 Applications of MR Fluid Based Finishing Processes

- Medical instruementation industries
- Defence industries
- Aerospace and automobile industries
- Optical industries etc.

Chapter 2 Literature Review

2.1 Literature Review

A large number of conventional and advanced finishing processes have been introduced by researchers as per requirement of surface finish surfaces and their application. Some of these processes [3] which are relevant to the present work are going to be discussed here. Traditional finishing process was developed to finish the workpiece to get required surface quality, such as grinding, honing, ball burnishing, etc [1]. However the requirement of nano level surface finish [6] was still an issue because of various reason like application in medical instrumentation, depending of efficiency of engine on the surface finish of piston cylinder, high temperature intending during finishing with available finishing methods, non-uniformity of the forces acting on the abrasive particles, etc. Therefore, to deal with these problem many of the advance finishing processes were developed. Development of magnetorheological finishing process is the most important step towards the development of advanced finishing process [17]. In this chapter literature review of various authors regarding the magnetorheological polishing fluid based finishing processes has done to understand the each and every aspect of these kinds of processes. Brief observations have been drawn from the various papers which are given below to better understand.

[Jain, 2008] discussed about all type of finishing process from tradition to advanced then magnetorheological abrasive based finishing process. To get rid of limitations involved in traditional finishing techniques the hybridized finishing process was developed which helped in increasing the capabilities of achieving absolute surface roughness values. This study offered the knowledge about suitability of finishing process for the given type of workpiece, for example advanced finishing processes which can be used for finishing up to nano level, are abrasive flow machining (AFM) used for complex shaped components, magnetorheological finishing (MRF) for complicated shape, small and medium sized components, magnetic float polishing (MFP) is implemented for spherical components, and magnetic abrasive finishing (MAF) process is used for large size, plane and cylindrical components. Therefore, this study enabled to opt the right process to finish the particular type of workpiece.

[Jha and Jain, 2004] developed a finishing process which was useful for the precision finishing of complex intricate geometry with the help of magnetorheological abrasive fluid. For study the performance of process and its feasibility experimentation set was developed which was hydraulically activated. The components of experimental set were MRP fluid cylinders, electromagnets, hydraulic actuators, fixture and supporting frame. Workpiece of Stainless steel material was used to perform experiments at different magnetic field strength to study the effect on final surface finish through the SEM images and roughness values. As the magnetic flux density was increasing the surface roughness was reducing it can be seen from the given below figure 2.1.

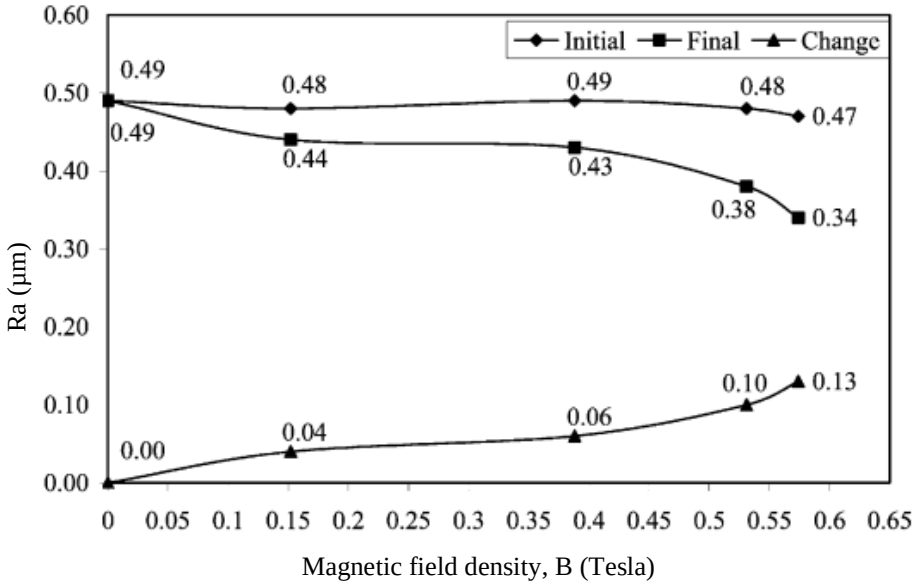

Figure 2.1: Relation of magnetic field density with roughness value Ra [5]

[Jayswal *et al.*, 2005] presented the theoretical survey on the magnetic abrasive finishing (MAF) process. This process was applicable for the flat and large sized workpiece. During MAF finishing process workpiece was placed in between the two poles of magnet and MRP fluid is kept in between the gap of magnetic pole and workpiece. Due to magnetic effect on MRP fluid a magnetic abrasive flexible brush (MAFB) was formed in the gap which acted as multipoint cutting tool. To estimate the magnetic forces distribution on workpiece surface a finite element model was introduced. Due to the edge effect magnetic forces relatively act higher at the near edge of magnetic pole. In this study the simulated result was compared with the experimental result and found acceptable for the finishing period of 4 min.

[Jha and Jain 2006] developed model of MRAFF process for theoretical evaluation of surface roughness values. Workpiece of stainless steel were used for the experimentation with various mixtures of amount of CIPs and SiC abrasive particles in MRP fluid in fixed volume concentration. The outcome of this study was surface roughness calculation model and chain structure. Forces on abrasives particles and change in surface roughness during the finishing operation were calculated using model developed. From this this study it was determined that significant improvement in change in surface roughness which was 0.32-0.09 µm with use of CIPs of CS grade with SiC abrasive particle of mesh size 800 as illustrated in given Table 2.1'

Table 2.1: The improvement in result of surface roughness [18]

Expt. No.	**CIP dia. (D_{CIP}) (µm)**	**SiC dia. (D_{SiC}) (µm)**	**D_{CIP}/ D_{SiC}**	**Initial Ra (µm)**	**Final Ra (µm)**	**∆Ra (µm)**	**%∆Ra**
1.	18.0 (CS)	19.00	0.95	0.32	0.09	-0.23	-17.87
2.	18.0 (CS)	12.67	1.42	0.28	0.17	-0.11	-39.28
3.	18.0 (CS)	7.50	2.40	0.31	0.23	-0.08	-25.80
4.	3.5 (HS)	19.00	0.18	0.26	0.23	-0.03	-11.54
5.	3.5 (HS)	12.67	0.28	0.28	0.24	-0.04	-14.28
6.	3.5 (HS)	7.50	0.47	0.25	0.24	-0.01	-4.00

[Das *et al.*, 2008] presented theoretical exploration about MRAFF to understand importance of process parameters involved in material removal process. In this study an effort had been put to investigate the flow through the fixture. In this paper, it had been tried to understand the mechanism of medium flow which flows through fixture with the help of FDM. The medium was assumed as Bingham plastic to find out stresses developed during the operation. Capillary viscometer was used to analyze the effect of magnetic field density on rheological behavior of finishing medium which is shown in figure 2.2. CFD simulations of MRPF flow was done to validate the result.

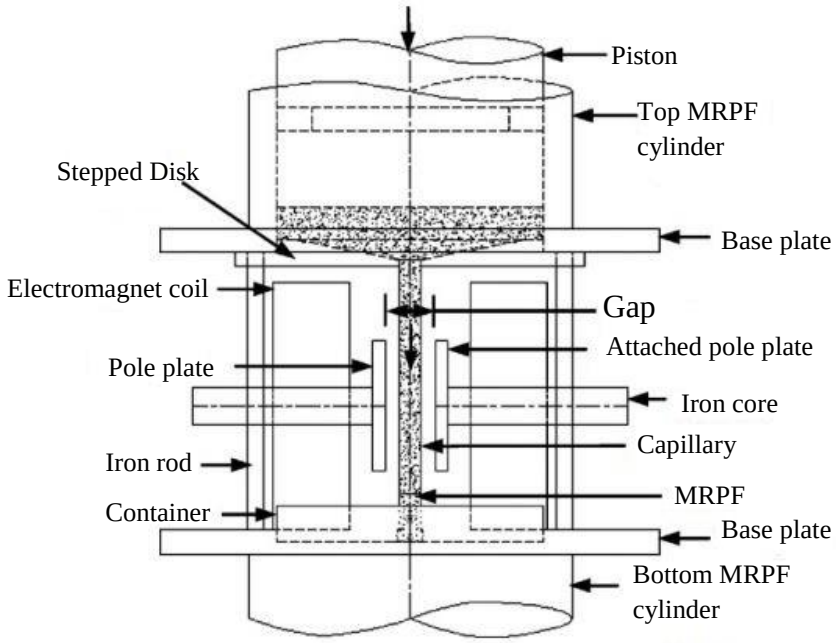

Figure 2.2: Capillary Viscometer [19]

[Schinhaerl *et al.*, 2008] investigated the forces involving in between the finishing tool and workpiece surface during magnetorheological finishing process. In this study the finishing process used, was computer controlled magnetorheological finishing process producing high quality of optical lenses. This process performs its function because of rheological behavior of MRP fluid through which the fluid changes its viscosity from liquid state to solid state in the presence of induced magnetic field. To measure the forces involving between MRP fluid and workpiece during finishing operation a three-axis dynamometer was used. In this paper variation of parameters experiences during performing the programme of experiment was discussed and some examples of variation of parameters was also given which are as shown in Table 2.2.

Table 2.2: Parameters involved in experiment and values used for the testing series [20]

Wheel (RPM)	Magnet (amps)	Pump (RPM)	Immersion depth (mm)
350	7	65	0.1
375	8	75	0.2
400	9	85	0.3
425	10	95	0.4
450	11	105	0.5
475	12	115	0.6
500	13	125	0.7

[Jain, 2009] presented an outline of numerous flowing abrasive based micro-nano machining (MNM) processes. Also proposed a universal mechanism of finishing technique for this process. All the processes discussed in as in advanced finishing processes were used medium and are externally controlled by magnetic field except two finishing process abrasive flow finishing (AFF) and electron emission machining (EEM). Therefore, through the control of magnetic field forces acting on abrasive particles and material removal was controlled. This study explored on the basis of experiment that why D.C. power supply pulse was used in MAF rather than smooth D.C. power supply.

[Sidpara and Jain, 2011] discussed different aspects of magnetorheological finishing process. With the help of experiment in magnetorheological fluid based finishing process forces involving in finishing action was examined. Through this study it was known that magnetorheological fluid based finishing processes were implemented for precise finish and for large variety of brittle material like optical glass, hard crystals etc. While experimentations dynamometer and other virtual instruments was implemented note the different forces acting on workpiece surface in the process. Variation of some factors affecting the process like rotational speed of wheel, concentration of CIP and abrasive by volume, and working gap was analyzed with respect to forces during experiment which is shown in figure 2.3.

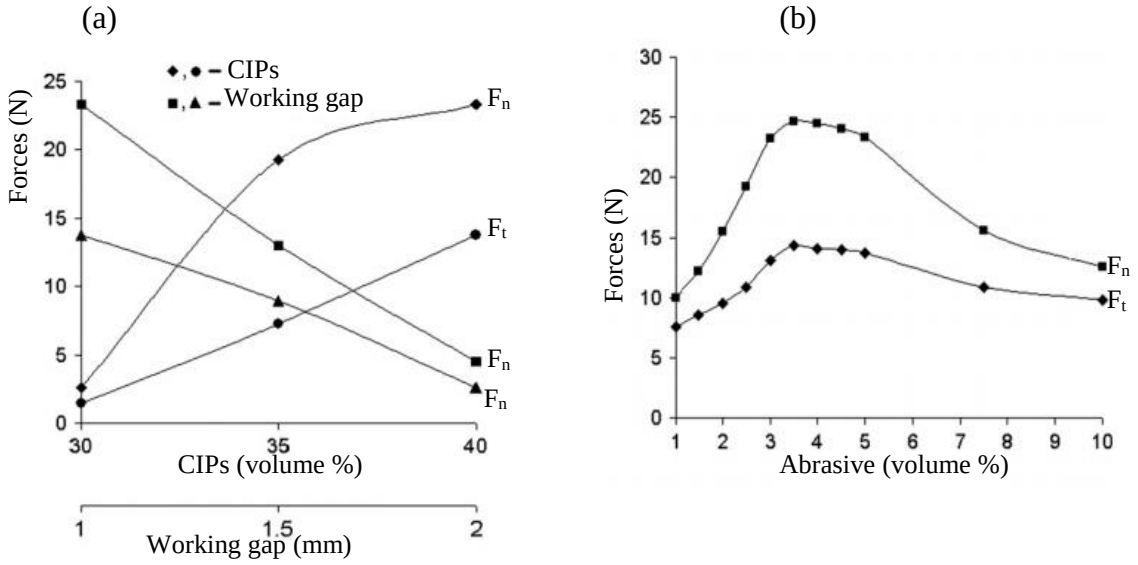

Figure 2.3: (a) Effect of carbonyl iron particle (CIPs) concentration and effect of work gap on tangential and normal force (CIPs is 40%, abrasive is 5%, wheel speed is 300 rpm) and (b) Outcome of concentration of abrasive on normal and tangential force (abrasive is 5%, working gap is 1 mm, wheel speed is 300 rpm) [21]

[Sidpara and Jain, 2012] utilized magnetorheological finishing to nano-level finish a blank single crystal silicon. The experimentation and plots were drawn to get the result and study the outcome of process parameters. In this study, it was studied that how to predict the consequence of process parameters involving in finishing process like concentration of CIP, concentration of abrasive particles, initial surface roughness, and carrier wheel speed on surface MRR during MR finishing process on single crystal silicon blank. The figure 2.4 shown below tells about the effect of lower concentration of abrasive on surface finish.

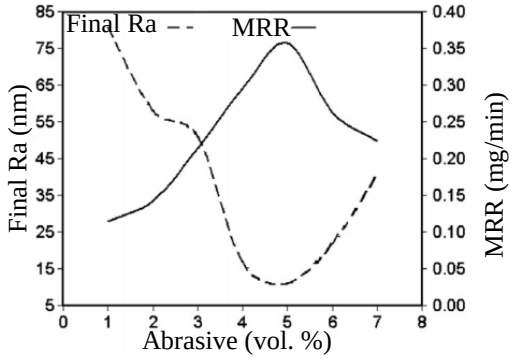

Figure 2.4: Effect of lower concentration of abrasive on final roughness and MRR (CIPs=40%, R=300 RPM, Rai=1250 nm) [22]

[Singh *et al.*, 2013] made an approach to know the material removal mechanism in ball end magnetorheological finishing process (BEMRF) on workpiece of ferromagnetic material. In this study model was developed for evaluation of magnetic field density as well as magnetic forces involving in BEMRF process with the help of measurements and observations of experiments. While modeling the magnetic normal force, some assumptions were considered because, it was difficult to understand mechanism of finishing with complex rotating MR-polishing. During this study scanning electron microscope (SEM) and atomic force microscope (AFM) was performed to clarify the mechanism of finishing action. Effect of variation of magnetic normal force was directly correlated with percentage change in surface roughness values during finishing as shown in table 2.3.

Table 2.3: Observation from experiments for the effect estimation of variation in Bz and Fn on % surface roughness change with working gap variation [23]

Sr. No.	Process Parameters			Experimental Results				
	N_t (RPM)	I (A)	Z (mm)	Bz (T)	Fn (N)	Initial Ra (µm)	Final Ra (µm)	ΔRa (%)
1	500	4	0.66	0.818	16.35	0.143	0.028	80.42
2	500	4	1.5	0.772	14.53	0.113	0.057	49.56
3	500	4	2.34	0.732	13.48	0.106	0.072	32.08

[Sidpara and Jain, 2013] attempted to understand how force are acting and impacting on freeform surface in case of magnetorheological finishing process. Being MR finishing process deterministic process for finishing plane, curved and freeform surfaces, well understand about the forces acting and their mechanism in different condition during finishing operation enhance the effectiveness of the process. To measure the forces on freeform surface during finishing operation in real time experimental examination was performed. Therefore, on the basis of experimental examination it was found that the normal forces dominated the other forces involved in the process. To validate the model experimental and theoretical results were compared and found the trends were in good agreement as shown in figure 2.5.

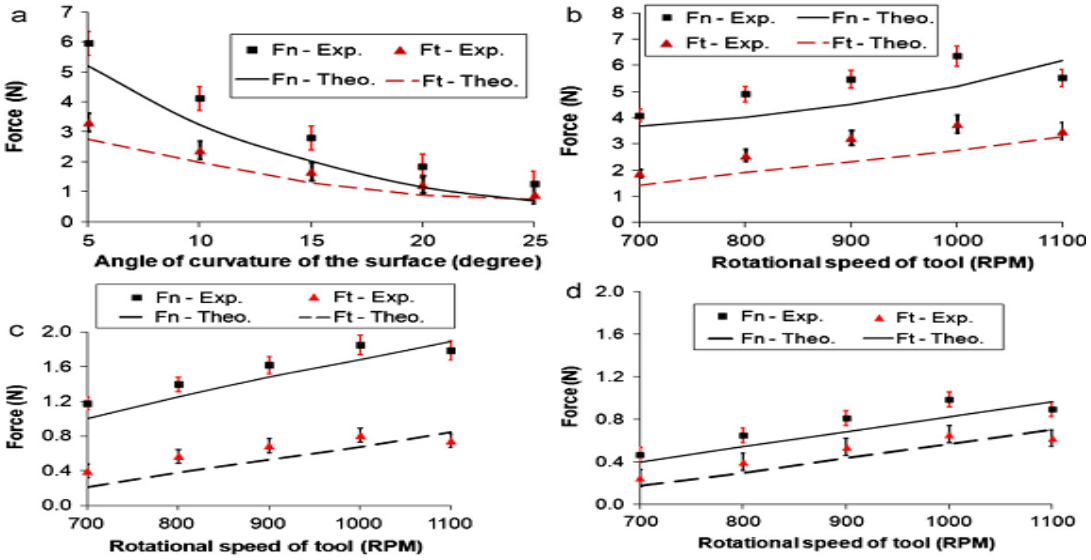

Figure 2.5: Comparative study of results in case of experimental and theoretical (a) angle of curvature of surface =1000 RPM and speed of rotation of tool at (b) $\theta=5^0$, (c) $\theta=15^0$ and (d) $\theta=25^0$ (■ and Δ signifies average values for the recurring experiments) [24]

[Kumar *et al.*, 2015] worked on the nano finishing of freeform surfaces by rotational magnetorheological abrasive flow finishing (R-MRAF) process. The objective of this study was to improve the exterior surfaces. The main principle used in the experiments of present study was large hydrodynamic pressure combined with magnetic fluid. The objectives of this process was fulfilled by reducing final surface roughness, by increasing uniformity of surface finish, and by enhancing finishing rate which were result of using MRP fluid having different mess size of abrasive particle and different exile pressure during finishing action was taking place. Improvement in the surface characteristics after the experiment performed is shown in figure 2.6.

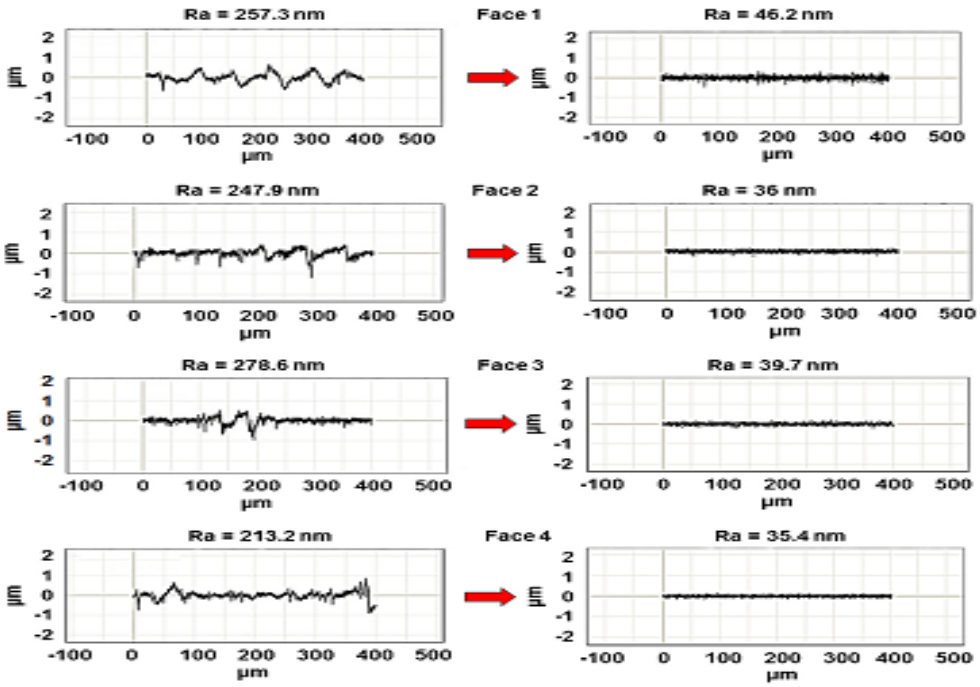

Figure 2.6: Surface roughness plots for the initial and final roughness (SiC abrasive mess size 2000, exile pressure 15 bar, operation cycles 1600, and rotational speed of magnet 150 rpm) [25]

[Wang and Hu, 2005] worked on magnetic abrasive finishing process for precise internal surface finishing of tube of 3 types of material Ly12 aluminum alloy, 316L stainless steel and H62 brass. This work was done under project sponsored by a pharmaceutical and mechanical company of Shanghai. The base medium used in finishing process includes 4% stearinic acid by weight percentage, and 96 % transformer oil by weight percentage. From the experimental observations it was concluded that finishing parameters like supply of magnetic abrasive, polishing speed, manufacturing process of magnetic abrasive and size of grains have serious impact on material removal rate.

[Sadiq and Shunmugam, 2009] developed the process for finishing the external curved surfaces, by giving rotational motion to the finishing tool and simultaneously pushing the magnetorheological abrasive fluid up and down was presented. Because of this type of relative motion in conventional honing process, this process was termed as magnetorheological abrasive honing process (MRAH). Important outline of present study can be seen in the figure 2.7.

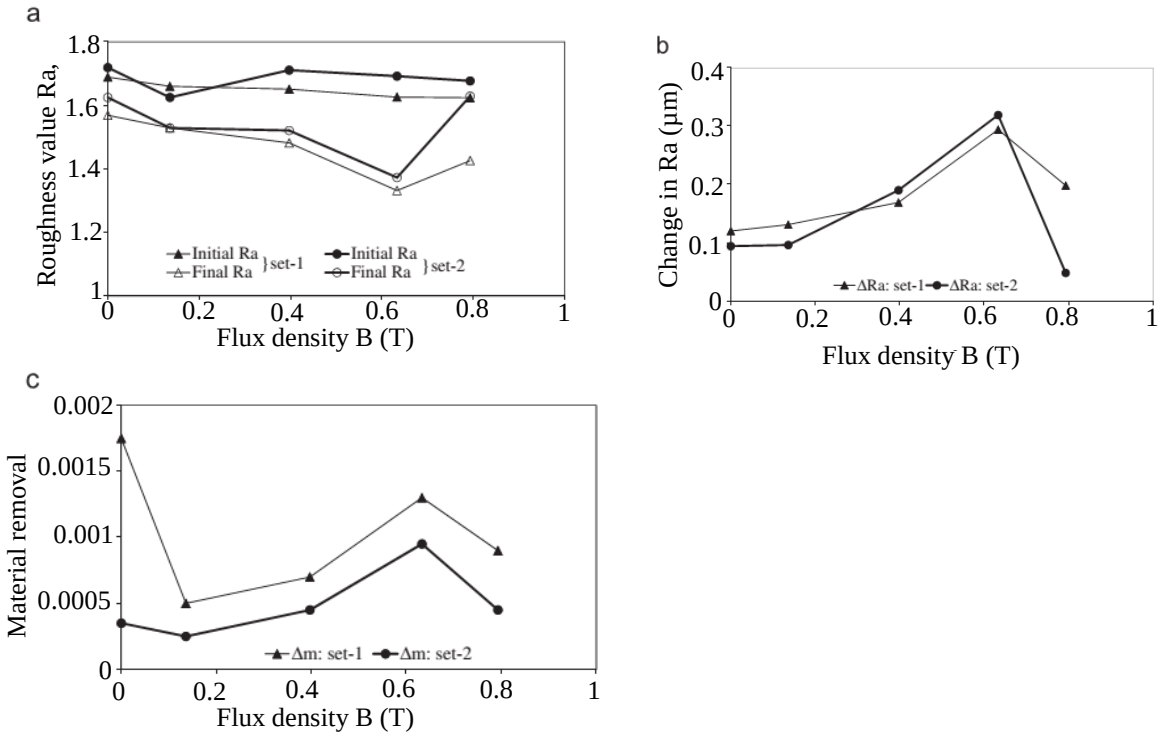

Figure 2.7: Impact of Magnetic field density on (a) surface roughness, (b) change in surface roughness and (c) material removal for aluminum samples (rotational speed: 450 rpm, reciprocation frequency: 15 cycles/min, time duration: 15 min) [27]

[Kang *et al.*, 2012] developed a finishing scheme having multiple pole-tip for finishing capillary tubes. To avoid several short steps for long tube by using single pole-tip, multiple pole-tip was used which reduced process time and to make more efficient rotational speed of tube is increased up to rotation 30000 min^{-1}. In this study, first of all finishing tool with double pole-tip was developed which confirms rotation of a tube up to 30000 min^{-1}. Second effects of speed of rotation and abrasives on the finishing performance were investigated. At last high speed finishing mechanism has been discussed in this article.

[Schmitt *et al.*, 2013] conducted a comparative study of different approaches to get a new approach to regulate automated honing process to achieve higher production accuracy and better process stability in shorter cycle time. The experiments were carried out on commercially available vertical honing machine LH30/300R by KADIA Produktion GmbH + Co. The material of workpiece used was hardened steel 16MnCr5. In this process before and after finishing workpieces were analyzed with a coordinate measuring machine, a roughness measurement device and a digital microscope. Three closed loop controller P1, P2, and P3 are used for regulating the process while experiments had carried out. The result of the study was

concluded as parallelism was better for P2 controller and straightness was slightly better for P3 controller. P2 and P3 controller provides the better results as compared to P1 controller.

[Judal *et al.*, 2013] presented a report on the development of a new vibration assisted cylindrical-magnetic abrasive finishing (VAC-MAF) setup and inspection of the involving several process parameter like vibration frequency, speed of rotational, abrasive particle size and density of magnetic field on the VAC-MAF setup while material removal workpiece of aluminum material. On applying this process it was concluded that the vibration frequency and abrasive particles size play a crucial role in improvement of the change in surface finish and material removal.

[Yamaguchi and Shinmura, 2004] developed a technique to finish the internal surface of alumina ceramic component, which was based on induced magnetic field. Through the experimentations on aluminum ceramic tube with consideration of different parameters process like effects of grains size of ferrous, volume of lubricant, and abrasive grain size material removal in this process was investigated. This process succeeds to get surface roughness values as 0.02 m fine and conveys insignificant additional enduring pressure to the workpiece surface. The Effect volume of lubrication on the finishing action and surface roughness value is shown as follows in given below figure 2.8.

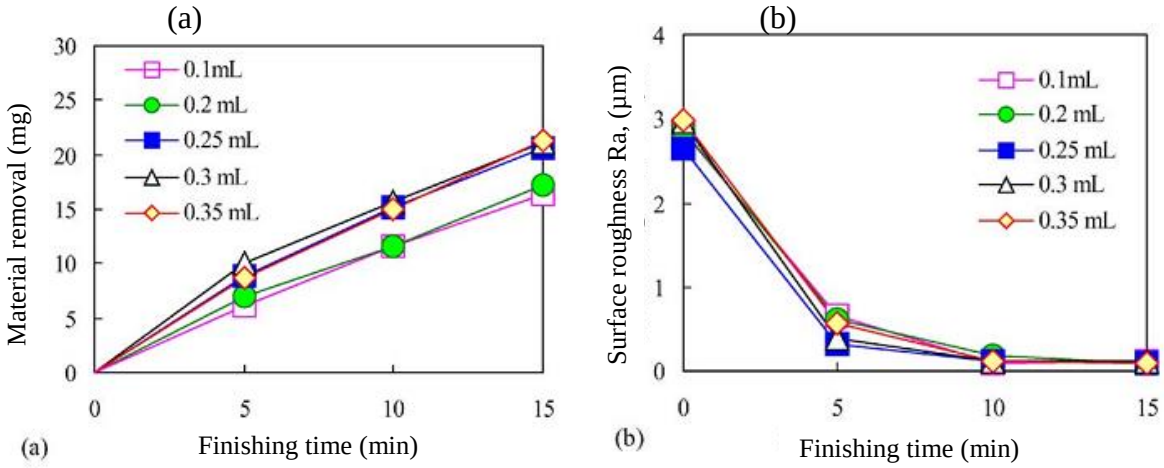

Figure 2.8: (a) Material removal vs finishing time and (b) surface roughness vs finishing time [31]

[Singh *et al.*, 2004] implemented Taguchi design of experiments to understand the factors effecting to surface quality. The parameters which influence the quality of surface finish during magnetorheological abrasive finishing were rotational speed of magnetic pole, abrasive size and working gap. During experimentation was found that change in surface roughness, working gap, voltage, mesh number of grain and rotational speed are some most notifiable parameters. To examine this process force transducer was developed to quantity force inducing during the process. Some important conclusions are shown in figure 2.9.

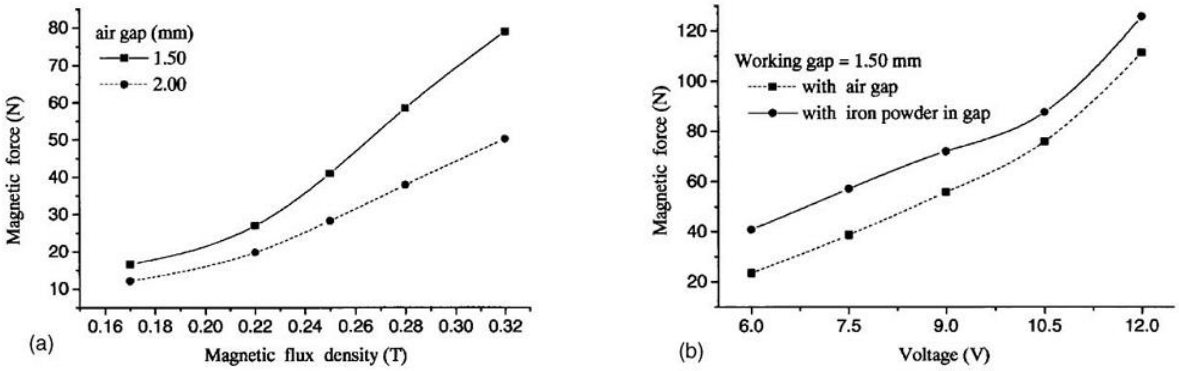

Figure 2.9: (a) Magnetic force variation against magnetic flux density at different working gap and (b) magnetic force variation against voltage in the following medium (i) working air gap (ii) working air gap filled with carbonyl iron powder [13]

[Jang *et al.*, 2013] studied about the mechanism of electrochemical magnetorheological polishing (ECMMRP) process which was applicable for the products made up of glassy carbon (GC) material. With the help of other conventional surface finishing process getting high quality of surface for the GC mold was challenging, owing this ECMMRP was developed. In this process film of oxide was formed on the surface of GC mold by applying over-potential to the specimen immersed in the electrolytic solution. Oxide film formed was quite softer than original mold material. Therefore, then the resulting mold was finished with MRP finishing process. In this article two experiments were conducted to understand the mechanism of finishing action in this process (1) potentiostatic and (2) electrochemical impedance spectroscopy (EIS).

[Misakian, 2000] developed the expressions of magnetic flux density for coplanar three rectangular loops. The magnetic flux density for loops with multiple numbers of turn were evaluated by multiplying the value calculated for single turn of loop or expression generated for the single turn of loop by the exact number turns in the system of coil. Also a quick program

for the expression was introduced in this paper to compute the magnetic field density at any arbitrary coordinate point.

[Niranjan and Jha, 2014] studied the bidispersed magnetorheological polishing fluid sample. The morphology of the prepared sample was seen through the scanning electron micrograph. Morphology of the sample can be seen in given below figure 2.10. From the figure it was concluded that the structure of CIPs were small spherical and irregular sizes whereas abrasive particle were of irregular shape and larger in size. With different combination of consisting components, four type of samples of MRP fluid were prepared as given in table 2.4. The rheology behavior of prepared samples was studied with the help of magntorheometer at different magnetic field strength.

Table 2.4: MRP fluid composition [34]

Sample Number	MR polishing Fluid Composition
Sample1 (Monodisperse)	20 volume % CIP of CS grade, 25 volume % SiC abrasive and 55 volume % base fluid.
Sample2 (Bidisperse)	18 volume % CIP of CS grade, 2 volume % CIP of HS grade, 25 volume % SiC abrasive and 55 volume % base fluid
Sample3 (Bidisperse)	16 volume % CIP of CS grade, 4 volume % CIP of HS grade, 25 volume % SiC abrasive and 55 volume % base fluid
Sample4 (Bidisperse)	14 volume % CIP of CS grade, 6 volume % CIP of HS grade, 25 volume % SiC abrasive and 55 volume % base fluid

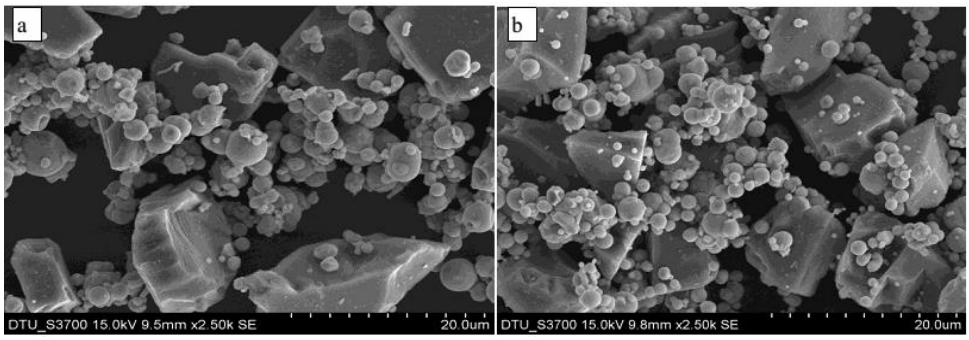

Figure 2.10: SEM images of (a) Monodisperse magnetic abrasives (sample 1) and (b) Bidisperse magnetic abrasives (sample 3) [34]

[Pattanayak and Aggarwal, 2014] developed a setup for the application of MRF using pillar drilling machine for finish the freeform surfaces of copper material. The effects of all involving process parameters like composition of MRP fluid, size of abrasives particle, rotational speed of workpiece, and vessel containing MR fluid, was studied. From this study it was concluded that improvement in surface finish on flat surface is better than cylindrical surface.

[Tricard *et al.*, 2006] presented a study on magnetorheological jet finishing process, which was very important to finish the optical surface with great extent of precision. In this literature theoretical and experimentally seen problem with conventional abrasive jet finishing was reduced. It was observed with results that MR Jet finishing can yield highly precised surfaces roughness value in nanometer from peak to valley is < 1 nm rms applicable for large numbers of material like advanced ceramics, single crystals, glasses and metals. The basic working principle can be understood from the figure 2.11.

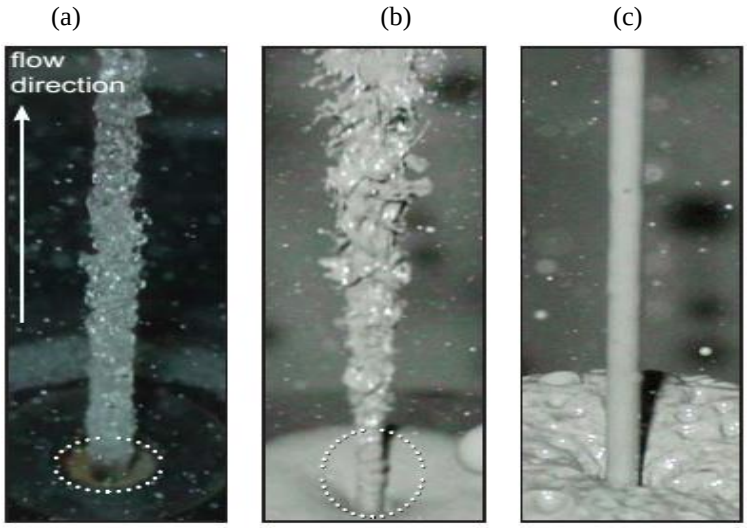

Figure 2.11: Snapshot image of Jet (velocity of flow = 30 m/s, dia. of nozzle 2 mm [36]

[Seok *et al.*, 2007] studied a method to fabricate curved surface on silicon centered microstructure assisted with magnetorheological finishing. In this study complete explanation was made for the procedure of fabrication of curved surface and investigation of surface features of workpiece during the production of the curved surface with assist of MR finishing. Several experiments were conducted under control and results were exhibited accompanied by its physical interpretation. To find curvature radius and roughness value of curved surface of workpiece RMS was applied.

[Sidpara *et al.*, 2009] conducted meticulous study to depict the rheological characteristics of MR fluid through design of experiment (DOE). During this study three models were used to depict the characteristics of the fluid which was Bingham Plastic, Herschel–Bulkley, and Casson fluid. To predict the volume of each component in the MR fluid response surface methodology (RSM) was implemented for estimation of saturation magnetization of the fluid, M-H curve was plotted with the help of vibrating sample magnetometer (VSM). Impact of temperature on yield stress was also discussed in this literature, it can be seen from the given below fig. 2.12.

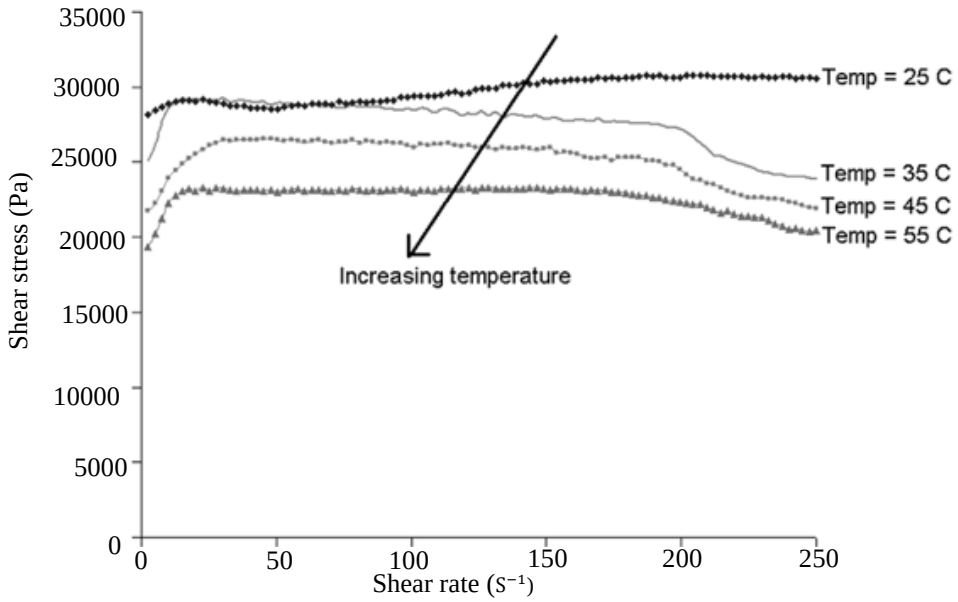

Figure 2.12: Consequence of temperature on yield stress and viscidity (CIP 38%, abrasive 4%, deionized water 52%, and magnetic field 06 T) [38]

[Gheisari *et al.*, 2014] introduced a new finishing process for finishing a cylindrical surface of aluminum material, using magnetorheological polishing fluid. In this study, three sets of experiments were conducted to predict the feasibility of finishing the cylindrical surface of specimen Aluminum using MR equipment. Complete study was divided in 4 sections, first section dealt with the introduction about the process, section 2 and 3 presented fundamental of MR finishing process, and the experimental setup respectively. Section 4 emphasized on the experiment procedure: firstly using variable workpiece speed, secondly testing variable process time, and thirdly evaluating the fast rectilinear alternating motion (RAM) effects in finishing process.

[Jung *et al.*, 2009] developed magnetorheological finishing process in which sintered iron-CNT compound was used as abrasive particles in MRP fluid and was capable to finish hard workpiece material. Generally MRP fluid was not applicable for finishing the hard material of Al_2O_3-TiC wheel type disk slider. On investigating theoretically as well as experimental it was found that decreased material removal rate in wheel type MR finishing process was due to mechanism of process. The two approaches for enhancement in rate material removal in this article was introduced first approach was rectilinear alternating motion to condition the processing environment, and second approach was enforcement to use more effective abrasives like iron powder sintered with carbon nanotube as shown in figure 2.13.

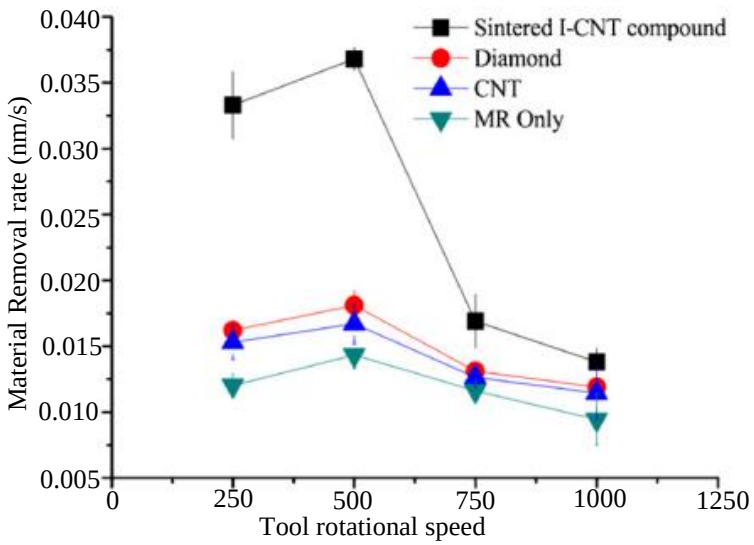

Figure 2.13: Variations of material removal rate against rotational speed of tool for four different types of abrasives [40]

2.2 Research Gap

From the reviewed literatures, the some research gaps have been found which are as follows:

- In all the existing MR fluid based finishing processes which were capable to finish the internal surface of cylinder, magnetic poles are kept outside of the workpiece. Therefore, due to such arrangement, carbonyl iron particles (CIPs) of magnetorheological polishing fluid stuck with the workpiece surface of magnetic material. The stuck CIPs with abrasive particles were unable to perform relative motion between the magnetic workpiece surface and active abrasives of magnetorheological polishing fluid which makes inefficient for finishing action on internal geometries of cylindrical ferromagnetic components. Due to stuck of CIPs with ferromagnetic internal surface, the existing MR fluid based finishing processes are limited to finish effectively only internal surface of non-magnetic workpiece.
- Recently, novel tool of magnetorheological (MR) honing process has been developed which is capable to finish internal surface of cylinder of magnetic as well as non-magnetic material. The advantage of this process is that finishing tool has been kept inside the workpiece. Therefore, the maximum magnetic field density gradient can be found at the tool core surface and lower at the surface of ferromagnetic or non-ferromagnetic workpiece. Since the magnitude of magnetic field in MRP fluid is significantly greater than the magnitude of magnetic field at workpiece surface in working gap, therefore, MRP fluid is more stiffened toward the tool core surface than

the ferromagnetic workpiece surface. Hence, MRP fluid is not stuck on magnetic workpiece and it can easily perform relative motion for the finishing action.

- The newly developed magnetorheological (MR) honing finishing process for internal surface of magnetic material has been improved for better performance and getting uniform finishing action as non-uniform variation in magnetic field has been noticed on its tool surface.
- There is no modeling and simulation for magnetorheological honing process tool has done so that one can develop new magnetorheological (MR) honing tool of any size for finishing the workpiece surface by varying the process parameter.

2.3 Objectives of the Present Work

The main objective of this present work is to mathematical modeling and simulation of the surface roughness of cylindrical workpiece in magnetorheological honing process for the improved magnetorheological honing tool. Therefore, to fulfill the main objective, the sub-objectives are as follows:

- To design the CAD model of the magnetorheological (MR) honing tool for better understanding while feasibility study of the tool and export the CAD model as IGES file for simulation of magnetic field through the Maxwell Ansoft software.
- To model the magnetic field induced in the gap between surface of tool core and inner surface of cylindrical ferromagnetic workpiece and calculate the theoretical values of magnetic field.
- To validate the magnetic field model with simulation of CAD model in Maxwell Ansoft software.
- To calculate the magnetic force acting on SiC abrasive particle with help of the calculated magnetic field in available magnetic force model.
- To calculate surface roughness values corresponding to different finishing cycles through the developed surface roughness model.
- To compare calculated surface roughness values with the experimentally surface roughness values for validating the developed model.

2.4 Methodology of Present Work

Methodologies for the present research work have been followed as per the following ways.

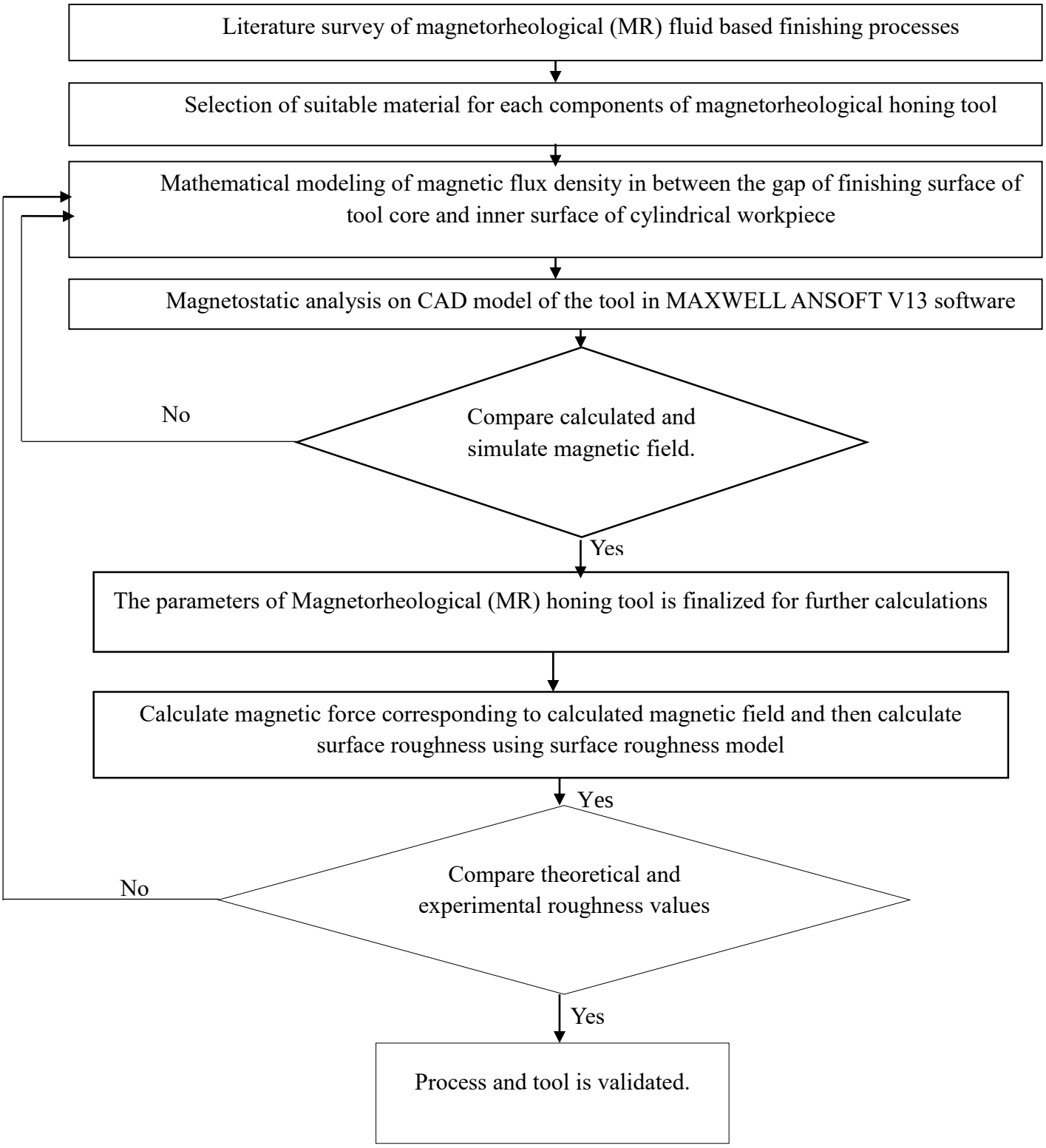

3.1 Limitations in Previous Magnetorheological (MR) honing tool

In recent study I-shaped magnetorheological (MR) honing tool has been developed for finishing the internal surface of ferromagnetic cylindrical workpiece. The design parameters considered in the present magnetorheological (MR) honing tool are the same parameters as considered in the design of I-shaped magnetorheological (MR) honing tool. The previous I-shaped magnetorheological (MR) honing tool had top and bottom spool type core and copper wire which was coiled in between the cylindrical inner core of the tool as shown in the figure 3.1.

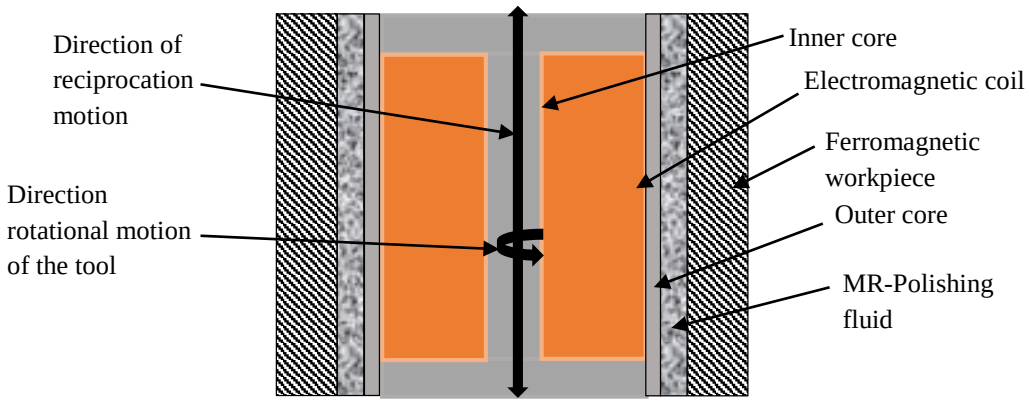

Figure 3.1: I-shaped magnetorheological (MR) honing tool

There are some limitations involved in previous I-shaped magnetorheological (MR) honing tool which are as follows:

Limitation in Efficiency: The previous magnetorheological (MR) honing tool was using electromagnetic coil in which the axis of rotational and reciprocation motion was perpendicular to the plane of electromagnetic coil. As the axis of tool motion was perpendicular to the loop of electromagnetic coil, the direction of magnetic lines were along the axis of reciprocating motion as shown in figure 3.2. Due to such arrangements of the tool abrasives could not apply the normal force on the workpiece surface therefore, that tool was found inefficient for the finishing process.

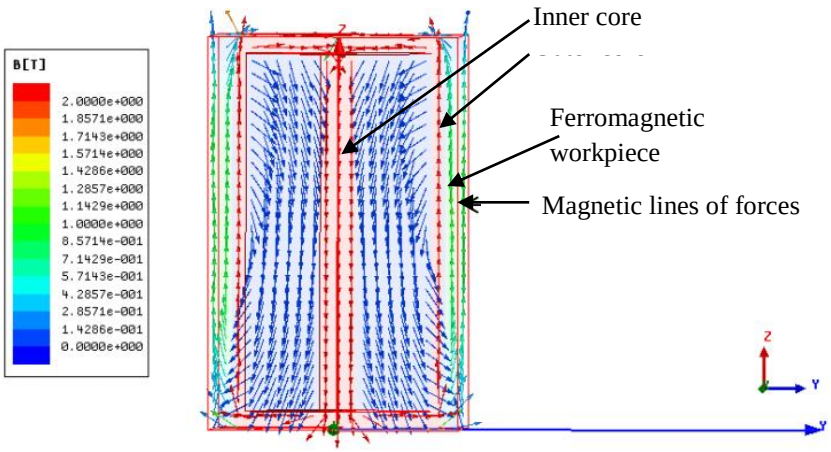

Figure 3.2: Direction of magnetic lines in magnetorheological (MR) honing tool

Takes more time for finishing operation: The I-shaped magnetorheological honing tool had 2000 number of turns of wires and used 4 A current, which caused to heat the tool very soon. Therefore, to avoid the burning of wire of coil large numbers of finishing step cycle has been introduced which took much more time for finish.

Lack of desired result of surface quality: From the simulation of I-shaped magnetorheological (MR) honing tool as shown in figure 3.2, the direction of magnetic lines is almost along the surface of workpiece. Due to such direction of magnetic line, SiC abrasives particles experience magnetic force in shear direction instead of normal direction which cause lesser indentation of abrasive into workpiece surface. Thus due to orientation of magnetic force during finishing action required surface quality could on achieved.

3.2. Experimental Setup and Tool Design

The design of this magnetorheological (MR) honing tool has done to improve the performance of finishing action in magnetorheological honing process. In this improved magnetorheological honing tool stiffened MRP fluid under induced magnetic field simultaneous performs rotational and translational motion along with the tool during finishing action. A schematic diagram of the improved magnetorheological honing finishing setup is shown in figure 3.3.

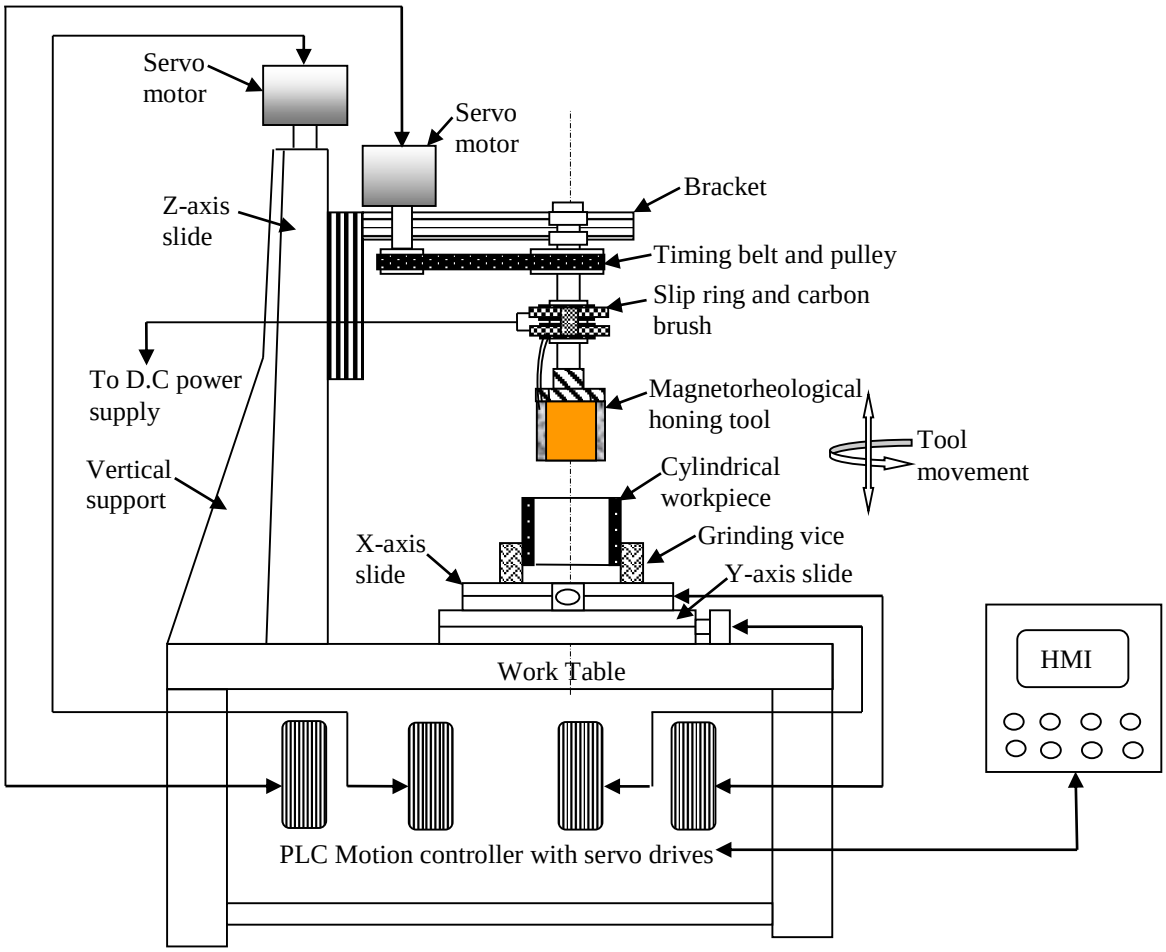

Figure 3.3: Schematic diagram of the PLC programme based computer-controlled machine with magnetorheological (MR) honing process setup

This magnetorheological honing process setup has vertically oriented magnetorheological honing tool which comprises of cylinder having three symmetric rectangular grooves, three separate rectangular core with curved surface which are in contact with MRP fluid, and rectangular electromagnetic coil (figure 3.4). The magnetorheological (MR) honing tool is positioned vertically on a vertical Z-slide such that the surface of tool core and the surface of a cylindrical workpiece can maintain gap of 1 mm for MRP fluid and can perform simultaneous translational and rotational motion along axis of vertical Z-slide. A motion controller is provided to precisely control the rotational and translational motion.

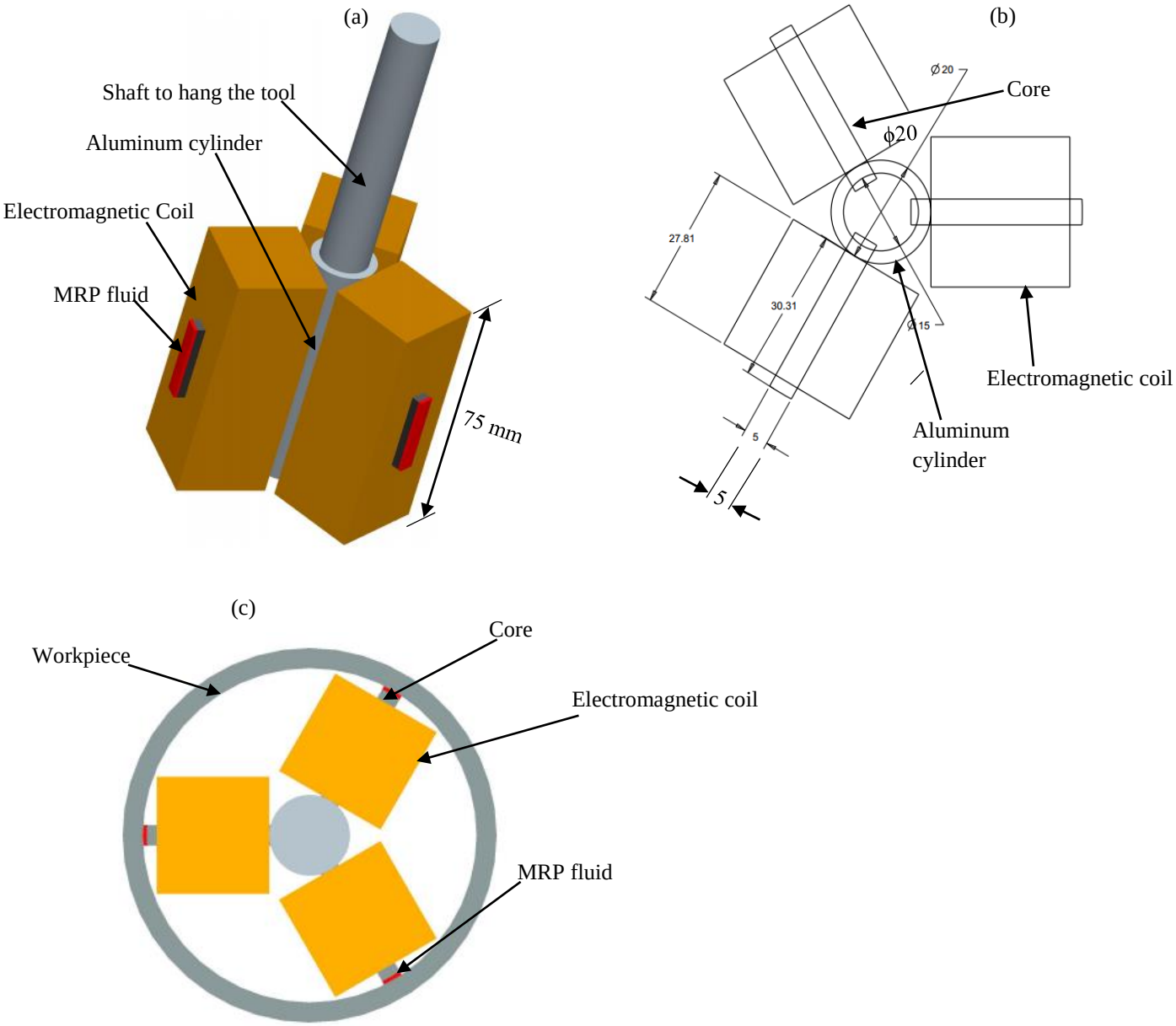

Figure 3.4: (a) Standard 3-D view of designed present magnetorheological (MR) honing tool (b) top frame view of the present designed magnetorheological (MR) honing tool and (c) Top view of present magnetorheological (MR) honing tool MRP fluid and workpiece

To hold the workpiece there is a platform fixed with X-Y linear movement slide. There are three stepper motor used to control linear motion of platform in X-Y-Z direction separately. Stepper motor used in X-Y is responsible horizontal motion of workpiece along X-Y plane, whereas Z motion controller is used for controlling vertical translational motion of magnetorheological (MR) honing tool.

3.3 Parameters of the Tool

The electromagnet coil has been designed to get maximum magnetic flux density at the surface of tool core of the magnetorheological (MR) honing tool. A comparative study of large number to designed tool based on dependent parameters such as number of turns, wire gauge, geometric factor and dimension of electromagnetic coil has been done. Using the studied parameters for design of tool simulation of magnetic field density in Maxwell Ansoft software was performed as shown in the figure 3.5. Therefore, on the basis of result of simulation performed the finalized parameters of the selected designed are as: number of turns of electromagnetic coil=700, maximum current to be assigned=1.5 A, copper wire gauge=23 SWG, geometry of electromagnetic coil is rectangular, dimension of the coil: inner length =25 mm, inner width =5mm, outer length=75 mm, outer width=29 mm, and the height (thickness due to lot of numbers of turns) of coil is 27.81 mm. Specifications of parameters assign to the software for Maxwell simulation are given below in the table 3.1.

Table 3.1: Specification of parameters used while simulation through Maxwell software

Specification	Material	Relative permeability	Current
Electromagnetic coil	Copper	1	1.5 A
Core	Mild steel	600	
MRP fluid	MR polishing fluid	5	
Workpiece	Mild steel	600	

The core of the tool is made up of mild steel material. The electromagnet coil is wound on the rectangular core of dimensional specification, length 25 mm, width= 5mm and height=30 mm. The magnetic field flows through core to MRP fluid filled in the gap of surface of tool core and inner surface of workpiece. MRP fluid delivery system comprises of a storage tank (funnel shape) along with speed controlled stirrer, manually formed MRP fluid is supplied to the magnetorheological (MR) honing tool for finishing operation.

3.4 Magnetostatic Simulation of Magnetorheological (MR) honing tool

The magnetostatic simulation has been performed for the designed tool of Magnetorheological (MR) honing tool (figure 3.4) using Maxwell Ansoft v13 software to assure the feasibility of the design for the purpose of finishing action. Through the magnetostatic simulation, distribution of magnetic field density on the tool and variation of the field density from the

surface of tool core to the inner surface of workpiece, has been observed. For optimization of dimensions of each component of the tool for accomplishing the maximum magnetic flux density on the outer tool core surface, the magnetostatic simulation has been done by varying the dimensions of each component. The optimized design is obtained on the basis of strength of magnetic field resulted corresponding to the same input parameters. The figure 3.5 (a) and (b) shown is the shape of magnetostatic simulated result of optimized tool, which has magnetic field density range 0 T to 0.65 T and direction of magnetic lines outward passing through the core of tool and normal to the workpiece surface.

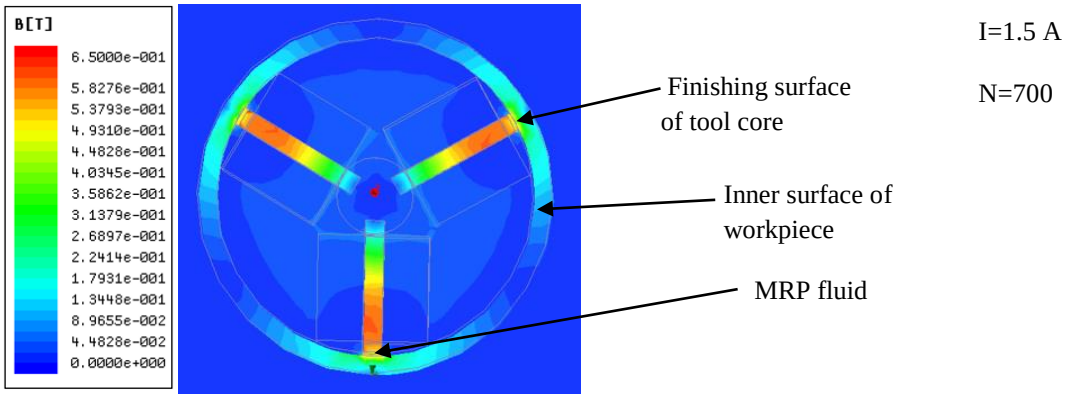

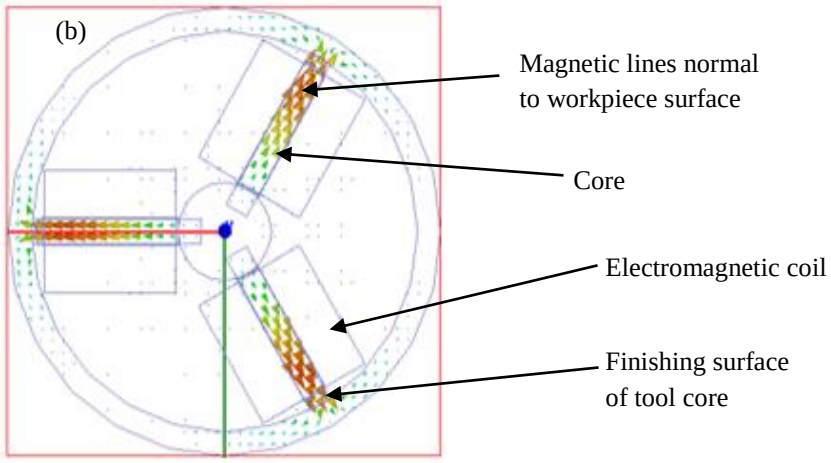

Figure 3.5: Magnetostatic simulation of (a) magnitude of magnetic flux density on the magnetorheological (MR) honing tool and (b) vector of magnetic flux density showing the directions of magnetic lines

4.1 Magnetorheological (MR) Honing Process and the Mechanism of Surface Finish

A schematic diagram of the magnetorheological (MR) honing Process setup is shown in Fig. 3.3 the setup is made in such a way that it enables simultaneous rotational and transaltional relative motion between the locked abrasive in CIPs chain structure and workpiece surface during process. In this setup, the cylindrical workpiece is fixed in the grinding vice and the magnetorheological (MR) honing tool (figure 4.1) is attached at tool holder, which is associated with timing belt and pulley. The two servomotors have simultaneous rotational and translational motions and these motions are controlled by programmable logic controller (PLC) program. As tool is attached with these two servomotors therefore, locked abrasive in between the CIP chains over outer surface of magnetorheological (MR) honing tool also have rotational and translational motions over the internal surface of cylindrical workpiece in helical path.

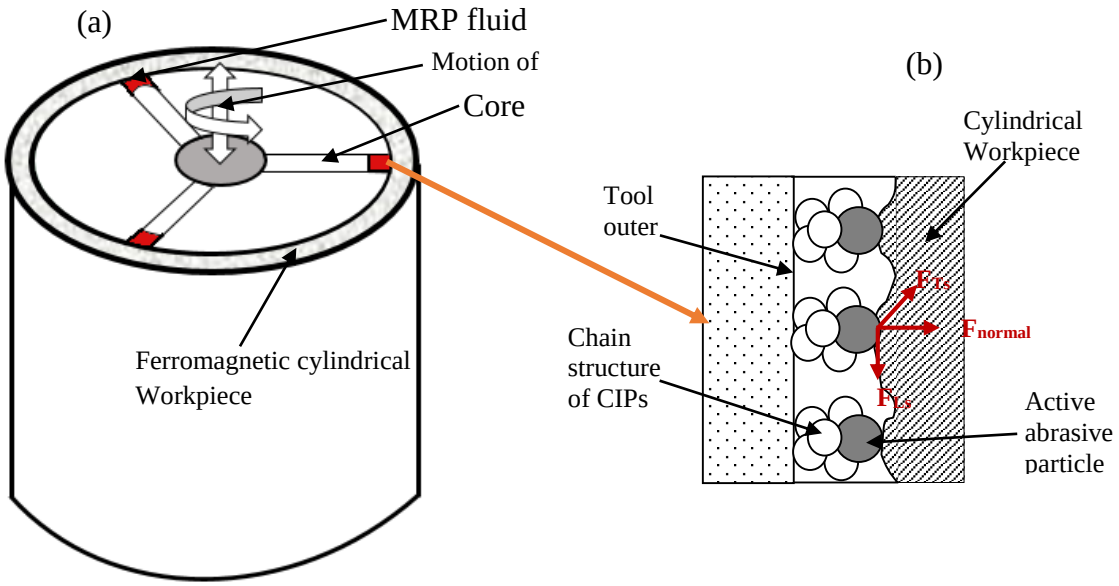

Figure 4.1: (a) Schematic of magnetorheological (MR) honing tool during finishing the internal surface of workpiece and (b) enlarged view of interaction of SiC abrasive particle and workpiece surface

Stiffness of MR polishing fluid on the magnetorheological (MR) honing tool surface depends on the rheological behavior of carbonyl iron particles in presence of magnetic flux density induced by electromagnetic coil. As current is applied to the electromagnetic coil, CIPs present in MRP fluid get aligned and make chain structures due to magnetic lines of induced magnetic flux density. Non-magnetic SiC abrasive particles of MRP fluid get locked in between the CIPs chain structures as shown in fig.4.1 (b). The abrasive particles, which are in contact with the workpiece surface are known as active abrasives particles. These active abrasives are cause for the material removal during simultaneous translational and rotational motion of a MRP fluid along with magnetorheological (MR) honing tool relative to workpiece surface. The constant contact and depth of indentation of active abrasives on the workpiece surface relies on the magnetic normal force (F_{normal}) whereas the longitudinal shear force (F_{Ls}) and tangential shear force (F_{Ts}) on abrasive due to simultaneous relative translational and rotational motions are the cause for material removal through wear action in microchips form during operation. Continuous change in position of active abrasive particle and continuous abrasive particle's motion relative to workpiece gives uniform surface finish.

4.2 Analysis of Magnetic Normal Force or Indentation Force

To understand the role of magnetic normal force in finishing mechanism and effect of magnetic field on the force in present process, it becomes necessary to develop mathematical model. The developed mathematical model can give complete understanding of the normal force, magnetic field and all other parameters involved in the finishing process. There are some basic assumptions have been taken into consideration for developing the model, which are as follows.

- All the abrasive particles are uniform in shape, size and uniformly distributed in the MRP fluid.
- All the abrasive particles are assumed spherical in shape and average diameter is 19 µm.
- All carbonyl iron particles are assumed as spherical in shape and average diameter of 18 µm.
- Gravitational forces, centrifugal force and inertial forces are neglected while finishing operation.
- Magnetic loses and leakages are not considered for the evaluation of normal force.
- Normal forces acting on active abrasive particles are responsible for indentation of abrasives into the workpiece surface and shear forces acting on the abrasives due to

simultaneous motions as rotational and translational, are responsible for the pull out of material from the surface of workpiece.

Shear force acting due to rotational and translational relative motion between the locked abrasives in CIPs chains and workpiece surface pull out the material from the workpiece surface in the form of microchips [9]. Due to the normal component of magnetic force acting on abrasive grains through carbonyl iron particles (CIPs), it creates groove into the workpiece surface. The indented groove corresponds to the profile of indented abrasive grains on the workpiece surface. Under the, shear force due to PLC controlled motion of magnetorheological (MR) honing tool with MRP fluid inside the cylindrical workpiece surface, the indented grains are given translational and rotational motion, which pulls out material from workpiece surface. The finishing action with abrasive particles takes place by shearing action or ploughing action, depending upon average cutting edge radius and depth of indentation [10]. There are no such evidences found either experimental or theoretical, which can tell about the actually finishing mechanism in the present magnetorheological (MR) honing process. Therefore, it has been assumed that normal component of all the forces acting on abrasive indents it into work surface, and shear component of all forces acting on it causes material removal in microchip form.

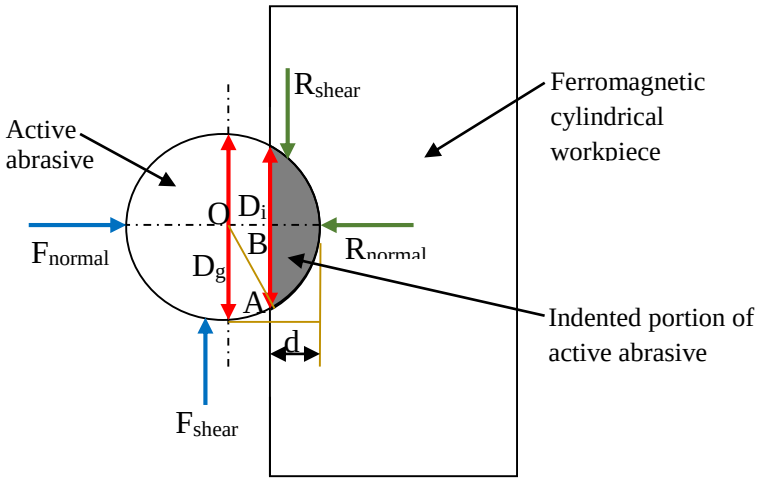

Figure 4.2: Forces implying on abrasive particle during magnetorheological (MR) honing operation.

The mechanism of material removal in the present process is shown in the fig.4.2, where normal force is applied due to the normal component of magnetic field through carbonyl iron particles. Here R_{normal} is the reaction force applied by the workpiece surface to resist indentation of abrasive particle on workpiece surface. If $F_{normal} > R_{normal}$, the indentation of abrasive particle

takes place [10]. F_{shear} is the shear force acting on the SiC abrasive particle due to tangential and translational motion MRP fluid along with the tool core relative to the workpiece surface. R_{shear} is the reaction force resisting to the deforming of grains of workpiece surface because of shear force. Therefore, for material removal, it is necessary to follow the condition $F_{shear} > R_{shear}$.

4.2.1 Calculation of MR Polishing Fluid and Chain Structures

The gap between the surface of tool core and workpiece is filled with magnetorheological polishing (MRP) fluid as shown in fig. 3.4 (c). To study the importance of MRP fluid in whole finishing mechanism, it is necessary study with all the facts about the fluid such as the volume of the fluid in the gap between finishing surface of tool core and workpiece surface, concentration of consisting component in MRP fluid and nature of each components of the fluid. The objective of this magnetorheological (MR) honing tool is to achieve nano finished internal surface of ferromagnetic cylindrical workpiece. Therefore, the surface of the tool core is taken circular shaped such that the active abrasives of MRP fluid in the gap uniformly interact with workpiece surface. Inner surface of cylindrical workpiece where MRP fluid is in contact, is taken of radius 41.31 mm as per designed tool setup, and gap between tool core surface and workpiece is of 1 mm that's why radius of surface of the tool core is taken 40.31 mm. The angle subtended by the arc formed by surface of the tool core at the centre of the tool is supposed to be θ, as shown in the figure 4.3.

Angle subtended by the surface of the tool core at the center:

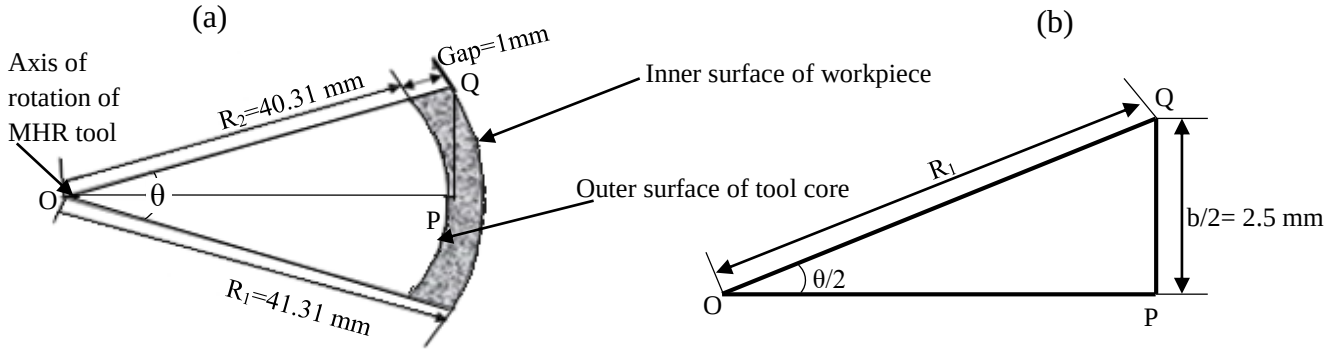

Figure 4.3: (a) Sector formed by MRP fluid layer in gap between tool core and workpiece surface and (b) right angle triangle formed with half of the sector

From the right angled triangle shown in figure 4.3 (b), on applying trigonometric relation, as given below

$$\sin\frac{\theta}{2} = \frac{Perpendicular}{Hypotenuse} = \frac{b/2}{R_1} \quad (1)$$

Therefore, angle subtended at the centre of tool by projected area in the gap of tool core and workpiece, $\theta = 6.9390^{\circ}$

$$Area\ of\ MRP\ fluid\ layer\ in\ gap, A = \frac{Angle\ subtended}{360}\pi(R_1^2 - R_2^2) \quad (2)$$

$$Total\ volume\ of\ MRP\ fluid\ in\ between\ gap\ of\ one\ core\ and\ workpiece,\ V_{MRF} = A \times H \quad (3)$$

Volume V_{MRPF} = 123.4975 mm^3 as taking height of core, H = 25 mm

$$Total\ volume\ of\ CIP\ particles\ present\ in\ the\ MRP\ fluid\ , V_{CIP} = \%\ volume\ fraction\ of\ CIP\ in\ MRP\ fluid\ \times\ total\ volume\ of\ MRP\ fluid \quad (4)$$

$$V_{CIP} = 2.469 \times 10^{-8} m^3 \quad (5)$$

$$Volume\ of\ single\ CIP, V_{sinle\_CIP} = \frac{4}{3} \times \pi \times (\frac{d_c}{2})^3 \quad (6)$$

where d_c is $diameter\ of\ a\ CIP\ particle$ and the value is $18 \times 10^{-6} m$

Therefore, $V_{sinle\_CIP} = 3.05208 \times 10^{-15} m^3$ (7)

$$Total\ number\ of\ CIPs\ in\ the\ volume\ V_{CIP} = \frac{V_{CIP}}{V_{sinle\_CIP}} = 8089566 \quad (8)$$

$$Maximum\ No.of\ CIPs\ occurring\ in\ a\ single\ chain\ structure\ = \frac{Gap}{Diameter\ of\ sinlge\ CIP} = 55 \quad (9)$$

$$volume\ of\ the\ CIPs\ in\ a\ single\ chain = total\ number\ of\ CIPs\ in\ a\ single\ chain \times V_{sinle\_CIP} = 1.678644 \times 10^{-13} m^3 \quad (10)$$

$$Mass\ of\ the\ single\ CIP\ = density\ of\ CIPs \times volume\ of\ the\ single\ CIP \quad (11)$$

where density of CIP is 7860 kg/m^3, therefore, $m = 2.3989 \times 10^{-11}\ kg$

4.2.2 Force Analysis

As carbonyl iron particles are magnetic in nature so under magnetic field there is a force induced by small magnetic CIP particle of mass m is given by eq. (12) [10].

$$F_m = m\mu_0\chi_m H\nabla H \quad (12)$$

where F_m is force on small ferromagnetic particle, m is the mass of a small CIP particle, χ_m is magnetic susceptibility of carbonyl iron particle, μ_0 magnetic permeability in free space and whose value is $4\pi \times 10^{-7}\ {}^{H}/_{m}$, H, is magnetic field strength, and ∇H is first derivative of magnetic field strength. Practically to use magnetic field strength the equation (12) can be written as equation (13) using $B = \mu_0 H$.

$$F_m = \frac{m\chi_m B \nabla B}{\mu_0} \tag{13}$$

Rectangular electromagnetic coil is a symmetric body. In the local coordinate system of the electromagnetic coil, sides of the coil are taken in X and Y axis direction and Z-axis of coordinate system is normal to the plane of the coil (X-Y plane). Due to side of rectangular coil symmetric along X and Y axis the magnetic force due to side of electromagnetic coil along X and Y axis cancel each other and results to zero but magnetic force in Z direction is added due to all the line current exerts force in a single direction leading to the non-zero magnetic force in Z direction. Therefore, the expression of magnetic force due to rectangular coil is expressed as in eq. (14).

$$F_m = \frac{m\chi_m B(z)\frac{\mathrm{dB(z)}}{\mathrm{dz}}}{\mu_0} \tag{14}$$

To calculate the magnetic force it is necessary to find out the involving term in the eq. (14) so magnetic susceptibility χ_m involving in eq. (14) is the degree to which a material can be magnetized in an external magnetic field and can be expressed as in eq. (15).

$$\chi_m = \frac{M}{H} = \frac{\mu_0 M}{B} \tag{15}$$

M-B plot is used for finding the characteristics (χ_m) of the CIP powder. M-B plot of the CI powder of CS grade is obtained by the VSM test [10] which is shown in fig. 4.4.

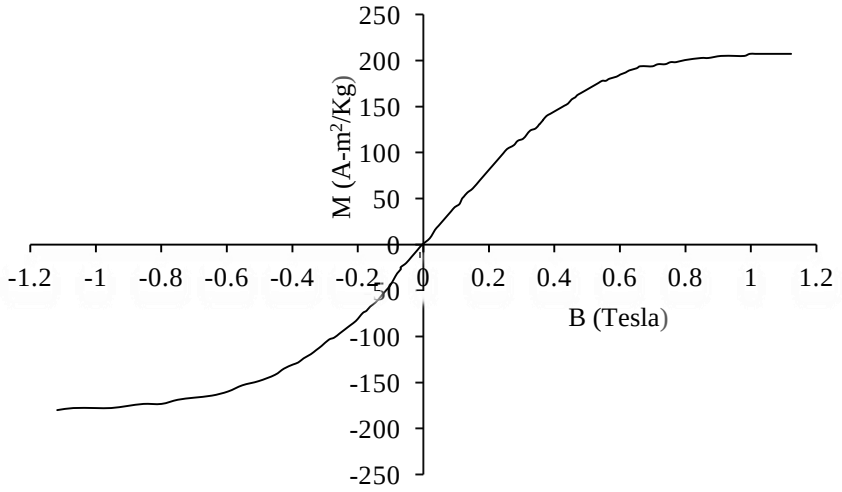

Figure 4.4: M-B curve of CIP of CS grade [10]

4.2.3 Mathematical Modeling of Magnetic Field in Present Magnetorheological (MR) Honing Tool Setup

In the present study, improved magnetorheological (MR) honing tool is made up of core of iron material having relative permeability (μ_r) 600 and electromagnetic coil has copper wire with 23 SWG (standard wire gauge). Since the core used in tool has rectangular geometry as already discussed in tool design section, electromagnetic coil is of rectangular shape. For the rectangular electromagnetic coil, local coordinate system is considered for mathematical modeling of the magnetic field induced in the gap of surface of tool core and workpiece surface. Therefore, the local coordinate system is shown in fig. 4.5 X-axis is along width of coil, Y-axis is along the length of coil, and Z-axis is taken along the height of the coil.

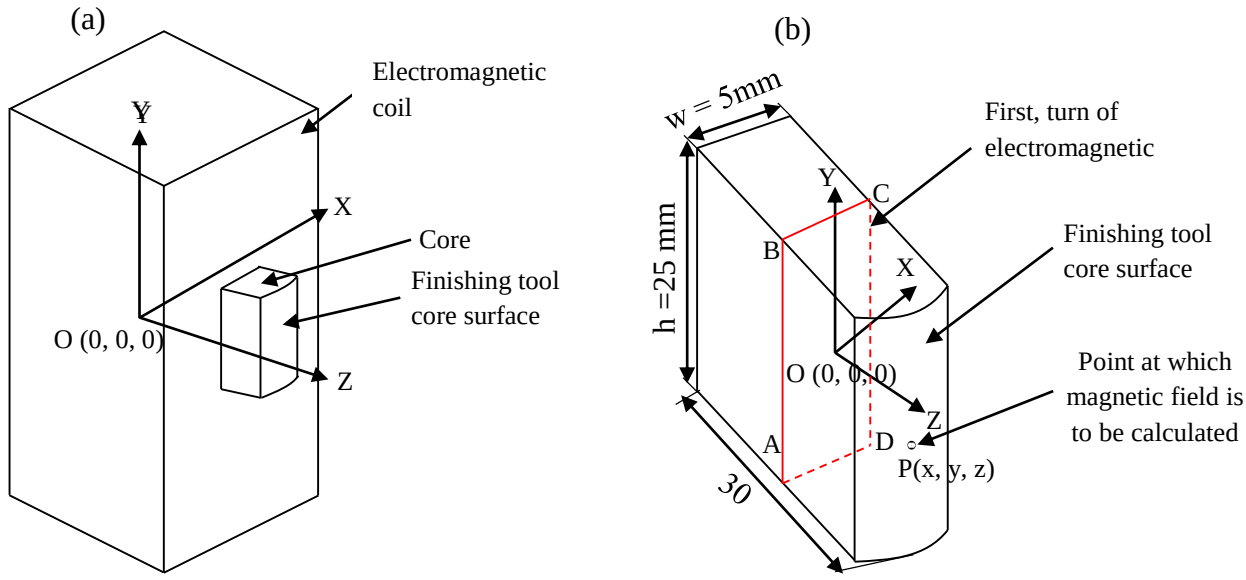

Figure 4.5: (a) Electromagnetic coil-core of magnetorheological (MR) honing tool and (b) core of magnetorheological (MR) honing tool

In present study, arrangement of electromagnetic coil and core of the magnetorheological (MR) honing tool is shown in figure 4.5 (a). The electromagnetic coil is consisting of magnetic mild steel core and 700 numbers of turns of 23 SWG on it. The first turn of electromagnetic coil is in direct contact with core and lying in XY plane of electromagnetic coil-core coordinate system at Z=0 position considered **[**33**]**. Dimensions of first turn of the coil, which has been considered for the derivations of magnetic field strength, are $w = 2a = 5\,mm,\ and\ \ h = 2b = 25\,mm$ as shown in figure 4.5(b). Electromagnetic coil turn ABCD as shown in fig. 4.5 (b) is considered for model the expression of magnetic field at point P(x. y, z) lying in between

the magnetorheological (MR) honing tool and workpiece. To model the magnetic field, strength Biot-Savart law for the line current is applied separately for each line segment of the coil. The Biot-Savart law for the line current passing through the linear conducting wire.

$$dH = \frac{I\vec{dl}\times\vec{R}}{4\pi R^3} \quad (16)$$

where *I* is current passing through the line segment, $\vec{dl}$ is elementary segment considered on the line, and $\vec{R}$ is position vector from considered elementary line segment to the point P(x, y, z) where magnetic field strength has to find out.

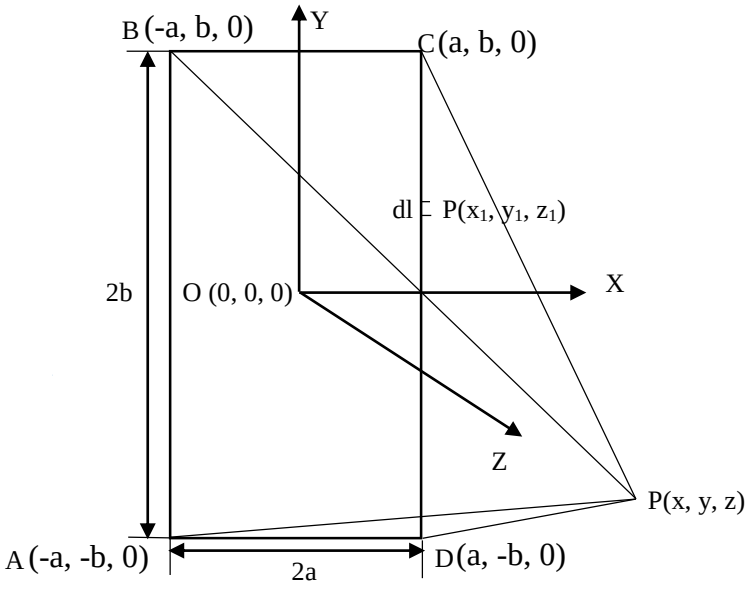

Figure 4.6: First turn of electromagnetic coil on the core

First turn of electromagnetic coil shown in fig. 4.6, shows AB, BC CD and DA are four line current segments of the coil. The point P (x_1, y_1, z_1) on the segment is the variable point at which magnetic field has to be calculated and it varies from 0 to the length of segment. Plane of first coil is taken in the XY plane of local coordinate system of the electromagnetic coil so the point P (x_1, y_1, z_1) has always value of z_1 is 0. To find out the magnetic field density at the point of P($x_1, y_1 z_1$,) due to current passing through the rectangular electromagnetic coil, Biot-Savart law is applied as eq. (16). Considering the AB segment of coil ABCD as shown in figure 4.7 and applying Biot-Savart law for find out the expression for magnetic field at the required point P($x_1, y_1 z_1$).

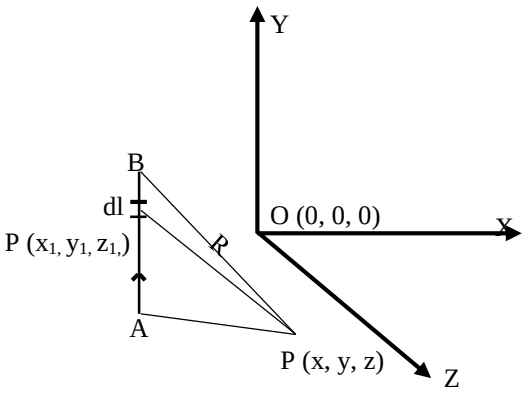

Figure 4.7: Line current passing through segment AB of turn ABCD

I current is passing through the wire segment AB, dy is the elementary line segment on conducting wire segment AB, $\vec{R}$ is the position vector of the point P (x, y, z) from the point on elementary line segment dy P ($x_{1,}$ $y_{1,}$ $z_{1,}$). With use of proper sign convention for the coordinate of point P ($x_{1,}$ $y_{1,}$ $z_{1,}$) x_1 is has negative sign because AB line segment is in negative X-axis, z_1=0 due to lying the first turn in X-Y plane, and as the segment is along the Y-axis from –b to b hence y_1 is taken as variable without sign and same approach is applied in remaining segments of first turn of coil. Therefore, using sign convention these vector quantities can be further expressed as in eqns. (17) and (18).

$$\overrightarrow{dl} = \overrightarrow{dy}\hat{j} \quad \text{and} \quad \vec{R} = (-x_1 - x)\hat{\imath} + (y_1 - y)\hat{\jmath} + (z_1 - z)\hat{k} \tag{17}$$

$$R = \sqrt{(-x_1 - x)^2 + (y_1 - y)^2 + (z_1 - z)^2} \tag{18}$$

Therefore, to find out $\overrightarrow{dl} \times \vec{R}$ cross product rule is applied and will get eq. (19) as below.

$$\overrightarrow{dl} \times \vec{R} = \{-(-x_1 - x)\hat{k} + (z_1 - z)\,\hat{\imath}\}dy \tag{19}$$

On applying eq. (17), (18) and (19) in eq. (16) the elementary effect of magnetic field strength at point P (x, y, z) due to elementary line segment dy is experienced, the expression is as in eq. (20).

$$dH_{AB} = I\frac{\{-(-\boldsymbol{x_1}-\boldsymbol{x})\hat{\boldsymbol{k}} + (\boldsymbol{z_1}-\boldsymbol{z})\,\hat{\boldsymbol{\imath}}\}\boldsymbol{dy}}{4\pi\{(x_1+x)^2+(z_1-z)^2+(y_1-y)^2\}^{\frac{3}{2}}} \tag{20}$$

To find out the magnetic field strength at point P (x, y, z) due to the complete line current segment AB, the eq. (20) is integrated over its coordinate value in which the considered elementary segment varies. Therefore, eq. (20) is integrated over –b to b (2b is height of the coil) and results to eq. (21). Here subscript AB on H signifies the magnetic field strength due to line current segment AB.

$$H_{AB} = I\frac{\{-(-\boldsymbol{x_1}-\boldsymbol{x})\hat{\boldsymbol{k}}+(\boldsymbol{z_1}-\boldsymbol{z})\,\hat{\boldsymbol{\imath}}\}}{4\pi}\int_{-b}^{b}\frac{\boldsymbol{dy}}{\{(x_1+x)^2+(z_1-z)^2+(y_1-y)^2\}^{\frac{3}{2}}} \quad (21)$$

On further solving the eq. (21), it results to eq. (22) as given below.

$$H_{AB} = I\frac{\{(x_1+x)\hat{k}+(z_1-z)\hat{\imath}\}}{4\pi\{(x_1+x)^2+(z_1-z)^2\}}\{\frac{b-y}{\sqrt{(x_1+x)^2+(z_1-z)^2+(y_1-y)^2}}+\frac{b+y}{\sqrt{(x_1+x)^2+(z_1-z)^2+(y_1-y)^2}}\} \quad (22)$$

Now taking next line segment BC, in which an elementary line segment dx is considered at the position P(x_1, y_1, z_1) for the calculation of magnetic field strength at the point P(x, y, z). The figure corresponding to current passing through the line segment BC is as shown below in figure 4.8.

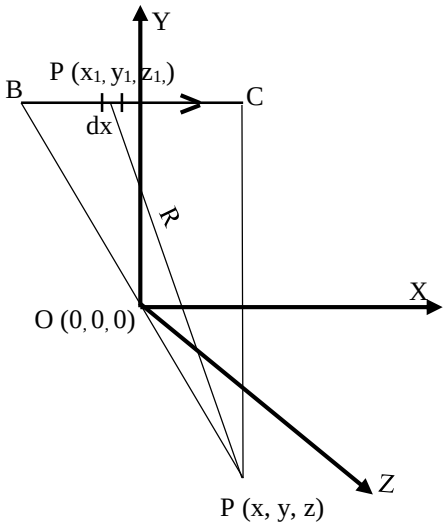

Figure 4.8: Line current passing through segment BC of turn ABCD

Since BC line segment is along X-axis therefore, the elementary line segment considered is $\overrightarrow{dx\hat{\imath}}$ and the sign convention is applied in same approach as applied for the segment AB. The involving terms in eq. (16) for line segment BC are as in eq. (23), (24) and (25)

$$\overrightarrow{dl} = -\overrightarrow{dx\hat{\imath}} \quad \text{and} \quad \vec{R} = (x_1 - x)\hat{\imath} + (y_1 - y)\hat{\jmath} + (z_1 - z)\hat{k} \quad (23)$$

$$R = \sqrt{(x_1 - x)^2 + (y_1 - y)^2 + (z_1 - z)^2} \quad (24)$$

Applying cross product vector rule on $\overrightarrow{dl}$ and $\vec{R}$ it results to eq. (25)

$$\overrightarrow{dl} \times \vec{R} = \{-(y_1 - y)\hat{k} + (z_1 - z)\,\hat{\jmath}\}dx \quad (25)$$

In similar to the steps done for line current segment AB, eq. (23), (24) and (25) are applied in eq. (16) and on further solving magnetic field strength at point P(x, y, z) due to current passing through line segment BC is

$$H_{BC} = I\frac{\{-(y_1-y)\hat{k}+(z_1-z)\,\hat{\jmath}\}}{4\pi\{(y_1-y)^2+(z_1-z)^2\}}\{\frac{a-x}{\sqrt{(x_1-x)^2+(y_1-y)^2+(z_1-z)^2}}+\frac{a+x}{\sqrt{(x_1-x)^2+(y_1-y)^2+(z_1-z)^2}}\} \quad (26)$$

Similarly for the line segment CD, elementary line segment dl is considered at the position P(x_1, y_1, z_1) for the calculation of magnetic field strength at the point P(x, y, z) as shown in fig. 4.9. Therefore, involving terms in eq. (16) for line segment CD are as in eq. (27), (28) and (29).

$$\overrightarrow{dl} = -\overrightarrow{dy}\hat{j} \qquad \vec{R} = (x_1 - x)\hat{\imath} + (y_1 - y)\hat{\jmath} + (z_1 - z)\hat{k} \tag{27}$$

Applying cross product vector rule on $\overrightarrow{dl}$ and $\vec{R}$ it results to eq. (28).

$$\overrightarrow{dl} \times \vec{R} = \{(x_1 - x)\hat{k} - (z_1 - z)\,\hat{\imath}\}dy \text{ and} \tag{28}$$

$$R = \sqrt{(x_1 - x)^2 + (y_1 - y)^2 + (z_1 - z)^2} \tag{29}$$

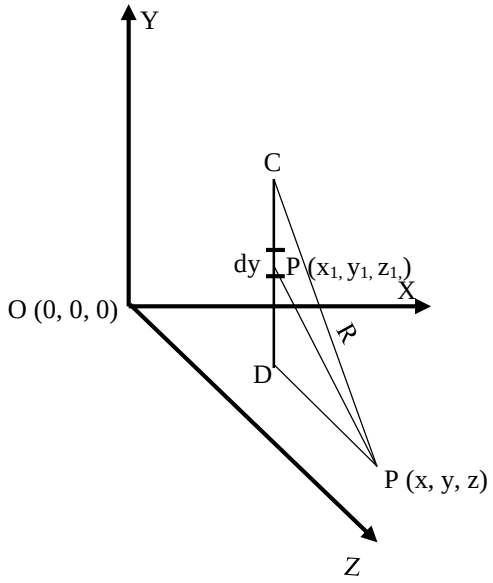

Figure 4.9: Line current passing through segment CD of turn ABCD

Similarly with the use of equations (27)-(29) in equation (16) and on further solving the magnetic field strength at point P(x, y, z) due to the line current of segment CD is:

$$H_{CD} = I\,\frac{\{(x_1-x)\hat{k}-(z_1-z)\,\hat{\imath}\}}{4\pi\{(x_1-x)^2+(z_1-z)^2\}}\left\{\frac{-(b+y)}{\sqrt{(x_1-x)^2+(y_1-y)^2+(z_1-z)^2}} - \frac{b-y}{\sqrt{(x_1-x)^2+(y_1-y)^2+(z_1-z)^2}}\right\} \tag{30}$$

Finally magnetic field strength due to line segment DA on the point of P(x_1, y_1, z_1).

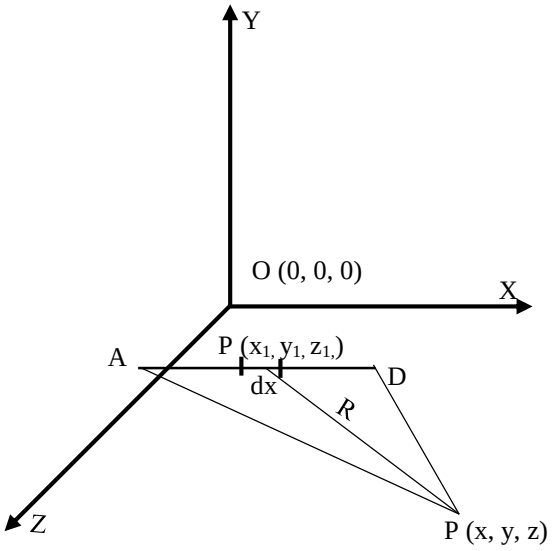

Figure 4.10: Line current passing through segment DA of turn ABCD

In similar way we will get the magnetic field strength at point P(x, y, z) due to the line current passing through line segment DA as shown in figure 4.10 is:

$$H_{DA} = I\frac{\{(y_1+y)\hat{k}+(z_1-z)\,\hat{j}\}}{4\pi\{(y_1+y)^2+(z_1-z)^2\}}\left\{\frac{-(a+x)}{\sqrt{(x_1+x)^2+(y_1+y)^2+(z_1-z)^2}}-\frac{(a-x)}{\sqrt{(x_1+x)^2+(y_1+y)^2+(z_1-z)^2}}\right\} \quad (31)$$

Therefore, the equations (22), (26), (30) and (31) are the magnetic field strength due to the line segments AB, BC, CD and DA respectively of rectangular coil ABCD at point P(x, y, z). The combined magnetic field strength due to all the four conducting line segment at the point P(x, y, z) is the sum of their separate effect of magnetic field strength. Therefore, the magnetic field strength due to rectangular coil at that point is:

$$H = H_{AB} + H_{BC} + H_{CD} + H_{DA} \quad (32)$$

On summing up the expression of magnetic field strength due to each segment of first turn of electromagnetic coil, the equation of magnetic field strength at the point P(x, y, z) becomes more lengthy. Therefore, to make easier to further analyze the equation is expressed separately according to the direction, as given in equations (33)-(35).

$$H_x = I\frac{(z_1-z)\hat{\imath}}{4\pi\{(x_1+x)^2+(z_1-z)^2\}}\left\{\frac{b-y}{\sqrt{(x_1+x)^2+(z_1-z)^2+(y_1-y)^2}}+\frac{b+y}{\sqrt{(x_1+x)^2+(z_1-z)^2+(y_1+y)^2}}\right\}+$$
$$\frac{-I(z_1-z)\,\hat{\imath}}{4\pi\{(x_1-x)^2+(z_1-z)^2\}}\left\{\frac{(b+y}{\sqrt{(x_1-x)^2+(y_1+y)^2+(z_1-z)^2}}+\frac{b-y}{\sqrt{x_1-x^2+(y_1-y)^2+(z_1-z)^2}}\right\} \quad (33)$$

$$H_y = I\frac{(z_1-z)\hat{\jmath}}{4\pi\{(y_1-y)^2+(z_1-z)^2\}}\left\{\frac{a-x}{\sqrt{(x_1-x)^2+(y_1-y)^2+(z_1-z)^2}}+\frac{a+x}{\sqrt{(x_1+x)^2+(y_1-y)^2+(z_1-z)^2}}\right\}-$$
$$\frac{I(z_1-z)\hat{\jmath}}{4\pi\{(y_1-y)^2+(z_1-z)^2\}}\left\{\frac{(a+x)}{\sqrt{(x_1+x)^2+(y_1+y)^2+(z_1-z)^2}}+\frac{(a-x)}{\sqrt{(x_1-x)^2+(y_1+y)^2+(z_1-z)^2}}\right\} \quad (34)$$

$$H_z = \frac{I(x_1+x)\hat{k}}{4\pi\{(x_1+x)^2+(z_1-z)^2\}}\left\{\frac{b-y}{\sqrt{(x_1+x)^2+(z_1-z)^2+(y_1-y)^2}}+\frac{b+y}{\sqrt{(x_1+x)^2+(z_1-z)^2+(y_1+y)^2}}\right\}+$$
$$\frac{-I(y_1-y)\hat{k}}{4\pi\{(y_1-y)^2+(z_1-z)^2\}}\left\{\frac{a-x}{\sqrt{(x_1-x)^2+(y_1-y)^2+(z_1-z)^2}}+\frac{a+x}{\sqrt{(x_1+x)^2+(y_1-y)^2+(z_1-z)^2}}\right\}+$$
$$\frac{I(x_1-x)\hat{k}}{4\pi\{(x_1-x)^2+(z_1-z)^2\}}\left\{\frac{-(b+y)}{\sqrt{(x_1-x)^2+(y_1+y)^2+(z_1-z)^2}}-\frac{b-y}{\sqrt{(x_1-x)^2+(y_1-y)^2+(z_1-z)^2}}\right\}+$$
$$\frac{-I(y_1+y)\hat{k}}{4\pi\{(y_1+y)^2+(z_1-z)^2\}}\left\{\frac{(a+x)}{\sqrt{(x_1+x)^2+(y_1+y)^2+(z_1-z)^2}}+\frac{(a-x)}{\sqrt{(x_1-x)^2+(y_1+y)^2+(z_1-z)^2}}\right\} \quad (35)$$

During solving the expressions of magnetic field strength, consideration of sign convention has been taken into account. Therefore, to find out the value of magnetic field strength only magnitude of coordinate point are used in the equations (33)-(35) of magnetic field strength for first turn of rectangular coil as x_1 =a; y_1 =b; and z_1 =0. In the study the point P(x, y, z) is on Z- axis, and it varies from the surface of the tool core to inner surface of workpiece therefore, x=0; y=0; and 15mm<=z<=16mm are taken for solving the expression. The main objective of this model is to calculate the magnetic field density in the gap between surface of tool core and inner surface of cylindrical workpiece due to n=700 turns of coil but from developed eq. (33)-(35) only magnetic field strength due to single turn of coil can be calculate. From the literature survey, it was found that numbers of turns can be multiplied in the field density of single turns of coil [33] and relation between magnetic field density B and magnetic field strength H is $B = \mu_0 H$. Therefore, magnetic field for n numbers of turns of electromagnetic coil is calculated from the eq. $B = n\mu_0 H$. Then on applying the complete information in equations (33)-(35) we can get the magnetic field as

$$\mathrm{B_x} = \frac{n\mu_0 \mathrm{I}(-\mathrm{z})\hat{\imath}}{4\pi\{(\mathrm{a})^2+(\mathrm{Z})^2\}}\left\{\frac{\mathrm{b}}{\sqrt{(\mathrm{a})^2+(\mathrm{z})^2+(\mathrm{b})^2}}+\frac{\mathrm{b}}{\sqrt{(\mathrm{a})^2+(\mathrm{z})^2+(\mathrm{b})^2}}\right\}+$$
$$\frac{-n\mu_0 \mathrm{I}(-\mathrm{z})\,\hat{\imath}}{4\pi\{(\mathrm{a})^2+(\mathrm{z}_1-\mathrm{z})^2\}}\left\{\frac{(\mathrm{b}}{\sqrt{(\mathrm{a})^2+(\mathrm{b})^2+(-\mathrm{z})^2}}+\frac{\mathrm{b}}{\sqrt{(\mathrm{a})^2+(\mathrm{b})^2+(-\mathrm{z})^2}}\right\}=0 \quad (36)$$

$$\mathrm{B_y} = \frac{n\mu_0 \mathrm{I}(-\mathrm{z})\hat{\jmath}}{4\pi\{(\mathrm{b})^2+(-\mathrm{z})^2\}}\left\{\frac{\mathrm{a}}{\sqrt{(\mathrm{a})^2+(\mathrm{z})^2+(\mathrm{b})^2}}+\frac{\mathrm{a}}{\sqrt{(\mathrm{a})^2+(\mathrm{z})^2+(\mathrm{b})^2}}\right\}-$$
$$\frac{n\mu_0 \mathrm{I}(-\mathrm{z})\hat{\jmath}}{4\pi\{(\mathrm{b})^2+(-z)^2\}}\left\{\frac{\mathrm{a}}{\sqrt{(\mathrm{a})^2+(\mathrm{z})^2+(\mathrm{b})^2}}+\frac{\mathrm{a})}{\sqrt{(\mathrm{a})^2+(\mathrm{z})^2+(\mathrm{b})^2}}\right\}=0 \quad (37)$$

$$\mathrm{B_z} = \frac{n\mu_0 \mathrm{I}(\mathrm{a})\hat{\mathrm{k}}}{4\pi\{(\mathrm{a})^2+(\mathrm{z})^2\}}\left\{\frac{4\mathrm{b}}{\sqrt{(\mathrm{a})^2+(\mathrm{b})^2+(\mathrm{z})^2}}\right\}+\frac{-\mu_0 \mathrm{I}(\mathrm{b})\hat{\mathrm{k}}}{4\pi\{(\mathrm{b})^2+(\mathrm{z})^2\}}\left\{\frac{4\mathrm{a}}{\sqrt{(\mathrm{a})^2+(\mathrm{b})^2+(\mathrm{z})^2}}\right\} \quad (38)$$

From the equations (36)-(38) magnetic field is calculated rectangular electromagnetic coil with use of dimensions of sides of rectangle as a=2.5mm, b=12.5mm and z is the distance on Z axis varying from 15mm to 16mm. To calculate the numerical values of the magnetic field strength, MATLAB program has been made. Here μ_0 is the magnetic permeability in space medium and value of magnetic permeability in space is $4\pi \times 10^{-7} T/m^2$. Magnetic permeability in any medium is calculated from the relative permeability which is defined as $\mu_r = \frac{\mu}{\mu_0}$, therefore, $\mu = 600 \times 4\pi \times 10^{-7} T/m^2$ has been taken as the relative permeability of iron core 600 **[**23**].** The magnetic field in the gap between surface of tool core and inner surface of workpiece calculated from MATLAB program is given in table 4.1.

Table 4.1: Magnetic field in gap between surface of tool core and inner surface of cylindrical workpiece at interval of 0.2 mm

Distance (mm)	Magnetic field B_X (T)		Magnetic field B_Y (T)		Magnetic field B_Z (T)	
	Theoretical (Eq. 36)	Using Maxwell software	Theoretical (Eq. 37)	Using Maxwell software	Theoretical (Eq. 38)	Using Maxwell software
15	0	0	0	0	0.3738	0.5012
15.2	0	0	0	0	0.356	0.4766
15.4	0	0	0	0	0.3391	0.452
15.6	0	0	0	0	0.3232	0.4274
15.8	0	0	0	0	0.3082	0.4028
16	0	0	0	0	0.2939	0.3782

From the data of magnetic field obtained as shown in table 4.1, it is observed that magnetic field density in X and Y direction due to the rectangular electromagnetic coil is zero because rectangular coil is in X-Y plane and current passing through coil is in X-Y plane. From the nature of magnetic field it is known that if current is passing through moving conductor then the magnetic lines pass through the perpendicular plane of current carrying conductor. Therefore in this case magnetic field along X-Y plane is zero and normal to X-Y plane has significant values. Another reason for the zero magnetic field in X and Y directions is due to the symmetric geometry of the electromagnetic coil, the effect of magnetic field effect is canceled out on each sides which results in zero magnetic field in X and Y directions.

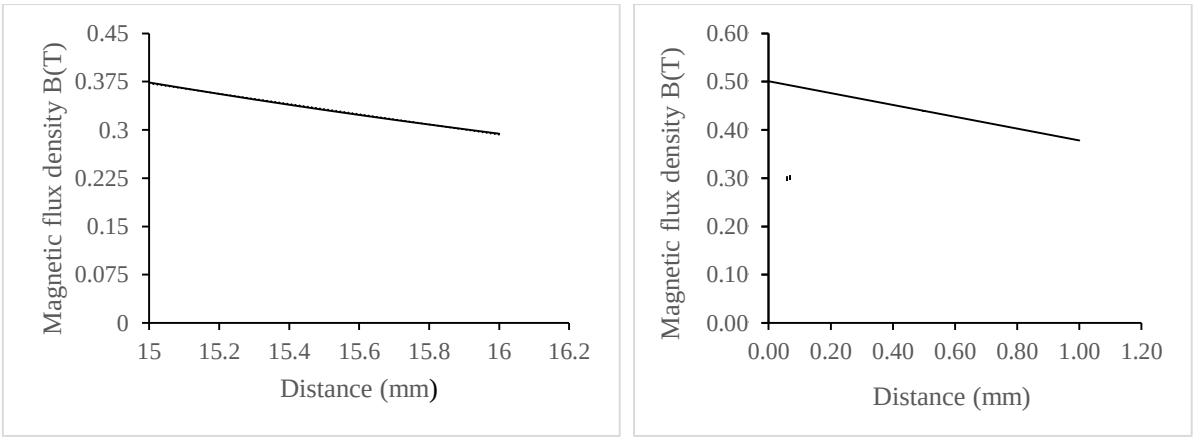

(a) (b)

Figure 4.11: (a) Theoretical variation of magnetic field in gap between surface of tool core and internal surface of workpiece and (b) variation of magnetic field in the gap using ANSOFT MAXWELL V13 software

Theoretically trend line followed by variation of magnetic field density in the gap between surface of tool core and workpiece surface is shown figure 4.11 (a) the equation corresponding to the trend line is:

$$B(z) = -0.0798z + 1.5697 \quad (39)$$

where z is position along Z-axis of local coordinate system where field density has to be calculated. For calculation of magnetic flux density (Tesla), unit of z is taken in millimeter. Derivative of equation of variation of magnetic field in gap is:

$$\frac{dB}{dz} = -0.079829 \quad (40)$$

Sign of $\frac{dB}{dz}$ is negative as shown in Eq. (40) which signifies the negative slope of magnetic flux density. The magnetic flux density is decreasing from the finishing surface of tool core to the internal surface of cylindrical ferromagnetic workpiece (Fig. 4.11). This trend of variation in magnetic flux density is desirable to avoid sticking of the carbonyl iron particles (CIPs) to the ferromagnetic workpiece surface. Due to this, it would not affect the relative motion between the stiffened MR polishing fluid and the internal surface of ferromagnetic workpiece. The schematic representation of the difference in magnetic flux density gradient between the finishing tool core surface and the internal ferromagnetic cylindrical surface.

On using all the relevant and calculated term in eq. (13) we will have the equation of magnetic force as in equation (41).

$$Fm = \frac{m\chi_m}{\mu_0}(-0.0798z + 1.5697)(-0.079829) \quad (41)$$

Mass of CIP particle is taken as $m = 2.3989 \times 10^{-11}\ kg$ which has been calculated from eq. (11). The mass of susceptibility of magnetic material is a function of magnetic field as expressed in equation (15). Therefore, using the calculated Magnetic field, and corresponding value of Magnetization from M-B plot (figure 4.4) χ_m is calculated as shown on table 4.2 and then average value of magnetic mass of susceptibility is calculated to use in calculation of magnetic force corresponding to the given magnetic field. The unit of magnetic mass of susceptibility is $m^3/_{kg}$ but distance of gap between tool core surface and workpiece surface is in millimeter. The average value of mass of susceptibility calculated in SI unit term is $\chi_m = 4.3666 \times 10^{-4}\ m^3/_{kg}$ and in millimeter the same magnetic mass susceptibility is given by. The magnetic force corresponding to the each magnetic mass susceptibility is calculated as shown in table 4.2.

Table 4.2: Calculated magnetic mass susceptibility of CIP and magnetic forces corresponding to magnetic field density in gap

Distance (mm)	Magnetic field density (T) (Eq. 38)	Magnetic mass of susceptibility (χ_m) × $10^{-4}\ mm^3/_{kg}$ (Eq. 15)	Magnetic force (F_m) × $10^{-10}N$ (Eq. 41)
15	0.3738	4.2000	-2.3937
15.2	0.356	4.2001	-2.2797
15.4	0.3391	4.3629	-2.2557
15.6	0.3232	4.5079	-2.2214
15.8	0.3082	4.4420	-2.0873
16.0	0.2939	4.4872	-2.0107

Here magnetic force is responsible factor for embedded SiC abrasive particles by CIP particles and also indent the active abrasive particle in the workpiece surface. Therefore, magnetic force is also considered as indentation force. The average value of calculated magnetic forces is taken for calculation of indention diameter of abrasive. This average magnetic force is termed here as indentation force and notified as F_i. From Eq. (40), it can be concluded that the derivative of magnetic flux density is negative which indicates the decreasing trend of magnetic flux density from finishing surface of tool core to the internal surface of ferromagnetic workpiece.

From Eq. (41), it clearly observed that magnetic flux density is in direct relationship with magnetic force/indentation force.

$$F_i = 2.2080 \times 10^{-10}\text{N} \quad (42)$$

4.2.4 Surface roughness modeling and simulation

Under the action of magnetic normal force on SiC abrasive particle through CIPs, it creates groove on the workpiece surface. The cross section of groove corresponding to the indented depth d, and the indentation diameter profile is as shown in given below figure 4.12, as hatched section. In the figure, D_g is the diameter of abrasive particle D_i diameter of indentation, d is the depth of indentation, F_{normal}, F_{shear}, R_{normal} and R_{shear} are the force acting on the abrasive particle tangentially and normal to the workpiece. F_{normal} is the force due magnetic field in z direction as per reference coordinate of coil, and R_{normal}, is the force reacting by the workpiece on the abrasive particle. Therefore, to indenting the grain it is necessary to F_{normal} should be greater than R_{normal}. F_{shear} is the force acting on abrasive particle due to rotational motion and translation motion given by servomotor to the tool. This force is responsible for the detaching grains of workpiece from the workpiece surface. As F_{shear} is greater than R_{shear} the material removal take place.

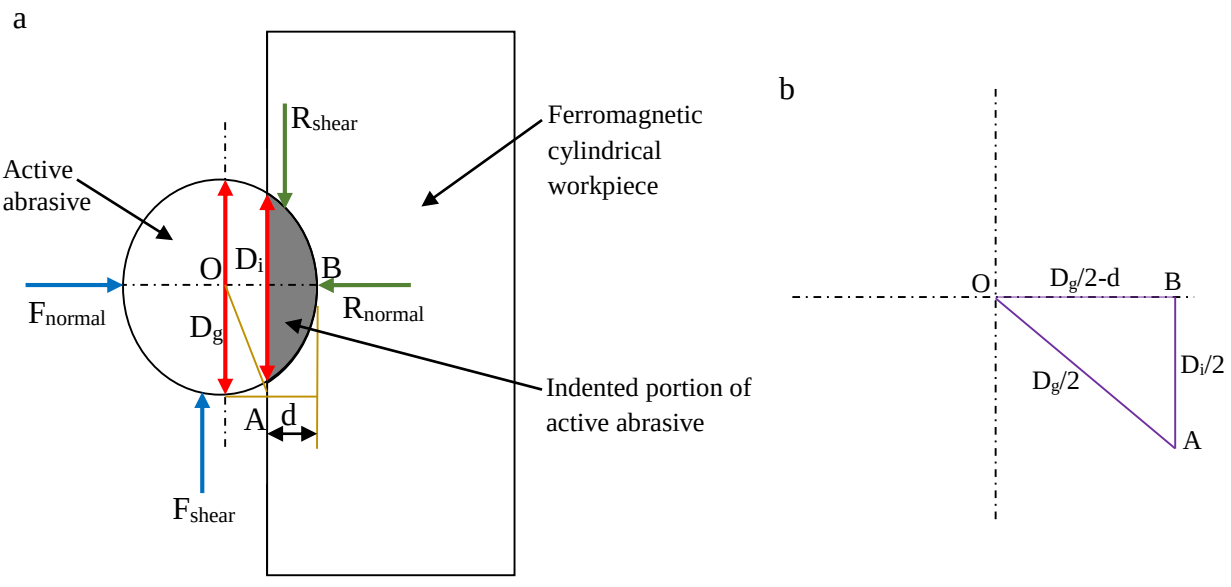

Figure 4.12: (a) Action of forces on abrasive particle in the process (b) OAB triangle formed due to indentation of abrasive particle

From the figure 4.12 (b) it is simple to understand that if any one of depth of indentation d and indentation diameter D_i is known then another one can be calculated by applying the Pythagoras theorem. The average value of depth of indentation is treated as average roughness of the surface. Relation between d, D_i, and D_g is as shown below.

$$d = \frac{D_g}{2} - \frac{1}{2}\sqrt{D_g^2 - D_i^2} \tag{43}$$

where D_g diameter of SiC abrasive grains which 19×10^{-6} m [15], and D_i is calculated from the relation of Hardness Brinell number. The Brinell hardness number kgf/mm^2 is defined as:

$$BHN = \frac{F_i}{A} \tag{44}$$

where F_i= force applied to the abrasive grian for indentating into workpiece surface;

and A=curved area of indentation= $\frac{\pi}{2} D_g (D_g - \sqrt{D_g^2 - D_i^2})$

Therefore, indentation diameter is calculated from the Brinell hardness number kgf/mm^2 equation on rearranging as in eq. (45).

$$D_i = \sqrt{D_g^2 - (D_g - \frac{2\times10^{-6}\times F_i}{9.8\pi H_{BHN} D_g})^2} \tag{45}$$

Here $D_g = 19 \times 10^{-6}\, m$ from the specification of material and for hardness testing of workpiece, experiment was conducted on the feroomagnetic mild steel workpiece specimen and it was found that hardness of workpiece was $BHN = 206$. Since it is a necessary for indent a grain into workpiece must be harder than the hardness of workpiec, therefore, hardness of abrasive grains in this study has been taken as hardness of workpiece. On applying the values of terms involved in eq. (45) value of diameter of indentation will be:

$D_i = 3.7326 \times 10^{-10} m$, and this value is on substituting in equation (43) the depth of indentation is calculated, which is $d = 1.83325 \times 10^{-15} m$.

Calculation of no. of active abrasive particle, N_g

Active abrasive particles are those abrasives which are in cantact with workpiece, and indentation on the workpiece surface is due to these abrasive particles. To finish the surface large number of active abrasive particle are required to indent into workpiece surface and pull out the material for finishing operation. Numbers of active SiC abrasives mesh size 800 present during finishing action, take responsibility of material removal during the finishing operation, and are calculated from the equation (46)

$$N_g = \frac{\%\ \text{Vol.fractionofSiCpartciles} \times \text{Area of internal surface of cylinderical workpiece} \times D_g}{\text{VolumeofsingleSiCparticle}} \quad 46)$$

where % volume fraction of abrasive particles is 20% ; A= area of MRP fluid layer between core and workpeice (calculated); D_g =diameter of single SiC abrasive particle which is 19µm; Volume of Single SiC particle, $V_{single\_SiC} = \frac{4}{3}\pi(\frac{D_g}{2})^3 = 3.589543 \times 10^{-15} m^3$ from the equation (6)

Total internal surface area of cylindrical workpiece= $2\pi R_1 H$ (47)

Therefre, number of active SiC abrasive particle calculated is equal to 357028288.

Let the workpiece used for finishing action, has initial roughness profile is as like shown in figure. In the figure 4.13 (a) Y_1, Y_2, Y_3, Y_4, Y_5 and Y_6 are the peaks and valleys on the initial surfcae surface. If N_g numbers of active abrasive particle per stroke indent depth d, then the resultant profile is Y_1', Y_2, Y_3', Y_4, Y_5' and Y_6' which is as shown in figure 4.13 (b). From figure 4.13 (b) it is clealy observed that the finishing action at valley positions doesn't take palce due to which before the start of next stroke, corresponding to valley profile initial reading is taking palce. Therefore, after completion of first stroke of finishing genralized representation of the profile is as given belwo in equation (48)

$$Y_i' = Y_i - N_g \times d \quad (48)$$

where 'i' subscripts on Y reperesnets the data points of roughness profile height; N_g is number of active abrasive particles and d is depth of indentation due to a single active abrasive particle.

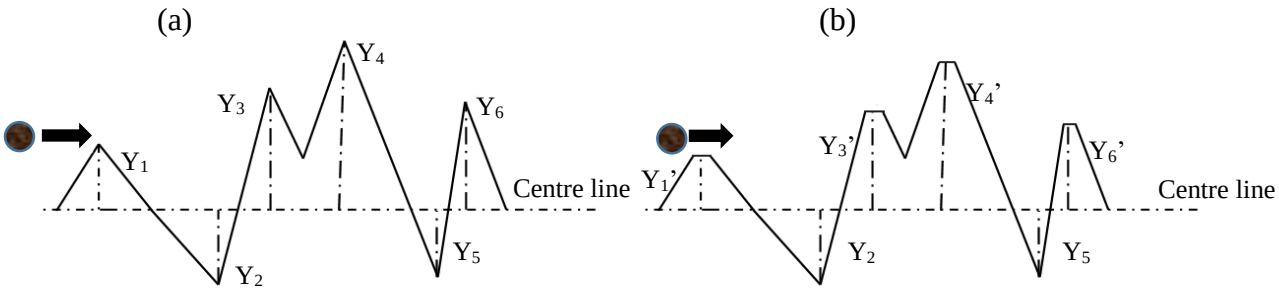

Figure 4.13: (a) Abrasive particles approaching initial height/depth and (b) new peak heights updated after one indentation depth [11]

The initial roughness profile data was measured with Mitutoyo SJ-400 surftest. All the sampled roughness profile data obatained from the surface roughness measuringinstruement were applied into the model with the help of MATLAB programme. After one stroke, the resultatnt roughness profile was as shown in figure 4.13 (b), profile Y_1 and Y_4 are same as initial because these are already below the centre line, hence only profile above the centre line were cutout and resultant to figure 4.13 (b). More clearly, it can be said that the peak values are checked from the sample data, and model was applied on it the data which are not peak that are proceed for next stroke by updating the new centreline. Again new peak data are operated and valleys data are sent for nex stroke operation by updating new centreline in this way the operation goes on till desired result is found. After and before the start of each stroke calculation new centre line average surface roghness values (R_a) is calculated from the previous profile data with the help of equation as below.

$$R_a = \frac{\sum_{1=1}^{N} |Y_i|}{N} \tag{49}$$

where N= number of profile data, Y_i = profile data at i^{th} position on workpiece surface.

While calculateing the new profile data through MATLAB programme of roughness it is assumed that continous removal of material takes place till the height of profile touches zero or non negative height after which no further material removal takes palce on that point. Because of assumption in theoretical calculation final data is either zero or very small positive height or valley height so further calculation is not possible on those resultant data. Therefore, for the each step of theoretcal calculation profile data is taken from the experimental data.

Theoretically magnetic flux densities in the gap between tip surface of core and workpiece were calculated from the derived equation (38) of magnteic field density for the electromagnetic coil. The calculated magnetic flux densities were used to calculated normal force or indentation force. Further the theoretically calculated indentation force is used calculate surface roughness as given bellow in table 5.1. To ensure the validity of mathematical model of this process and tool designed in present study, there are two checks in this study to has been developed , first check is comparison of theoretically calculated magnetic field density with simulated magnetic field in Maxwell Ansoft V13 software as shown in figure 3.3 (a). Second check of model is comparison of theoretically calculated surface roughness with the experimental values as shown in table 5.1. In the table % error column shows how deviation in surface roughness from experimental value to the theoretical value. Therefore, % error [14] is given as

$$\frac{(Experimental\ roughness\ value - theoretical\ roughness\ value)}{experimental\ (R_a)} \times 100 \quad (50)$$

Number of cycle

$$\text{Reciprocating velocity of medium in workpiece region} = \frac{2\times\text{workpiece height}}{\text{Cycle time}} \quad (51)$$

where, reciprocation velocity is taken as 50 cm/min, and workpiece height is 13 mm. Therefore, the calculated cycle time = 3.12 seconds.

$$\text{Number of Cycle} = \frac{\text{Total duration of finishing operation}}{\text{Cycle time}} \quad (52)$$

Observation for the effect of magnetic normal forces on surface roughness

The change in surface roughness profiles during different finishing cycles are shown in Figs. 5.1 (a-d). The profile data of surface roughness profile data measured from Surftest SJ-400 roughness tester were applied into the mathematical model in order to calculate the final change in surface roughness by using a MATLAB programme. The theoretically calculated surface roughness value was found as 0.40 µm while experimental roughness value was 0.41 µm with the first 450 finishing cycles. In next 600 finishing cycles, the theoretical roughness value was found as 0.32 µm while experimental roughness value was 0.34 µm. With the final 780 finishing cycles, the theoretical surface roughness was found as 0.23 µm, while experimental roughness value was 0.22 µm. Therefore, it was clearly observed that the experimental surface

roughness from initial 0.77 µm of surface roughness reduced to 0.22 µm and theoretically, the reduced value of surface roughness is 0.23 µm, which shows a significant change (approx. 70%) in surface roughness values. The changes of approximately 71.42% (experimentally) in surface roughness from initial surface roughness to final surface roughness clearly revealed that the theoretical and experimental results are in closer agreement with each other. In Table 5, the % error column shows how deviation in surface roughness from the experimental value to the theoretical value takes place. Therefore percentage (%) error can be calculated from the given Eq. (50) [23],

Table 5.1: Theoretical and experimental results of surface roughness corresponding to the number of cycle

Sr. No	Number of cycles	Experimental R_a (µm)		Theoretical R_a (µm)		% Error
		Initial R_a (µm)	Final R_a (µm)	Initial R_a (µm)	Final R_a (µm)	
1	0	0.77	0.77	0.77	0.77	0
2	160	0.77	0.41	0.77	0.40	2.43
3	185	0.41	0.34	0.41	0.32	5.88
4	210	0.34	0.22	0.34	0.23	-4.54

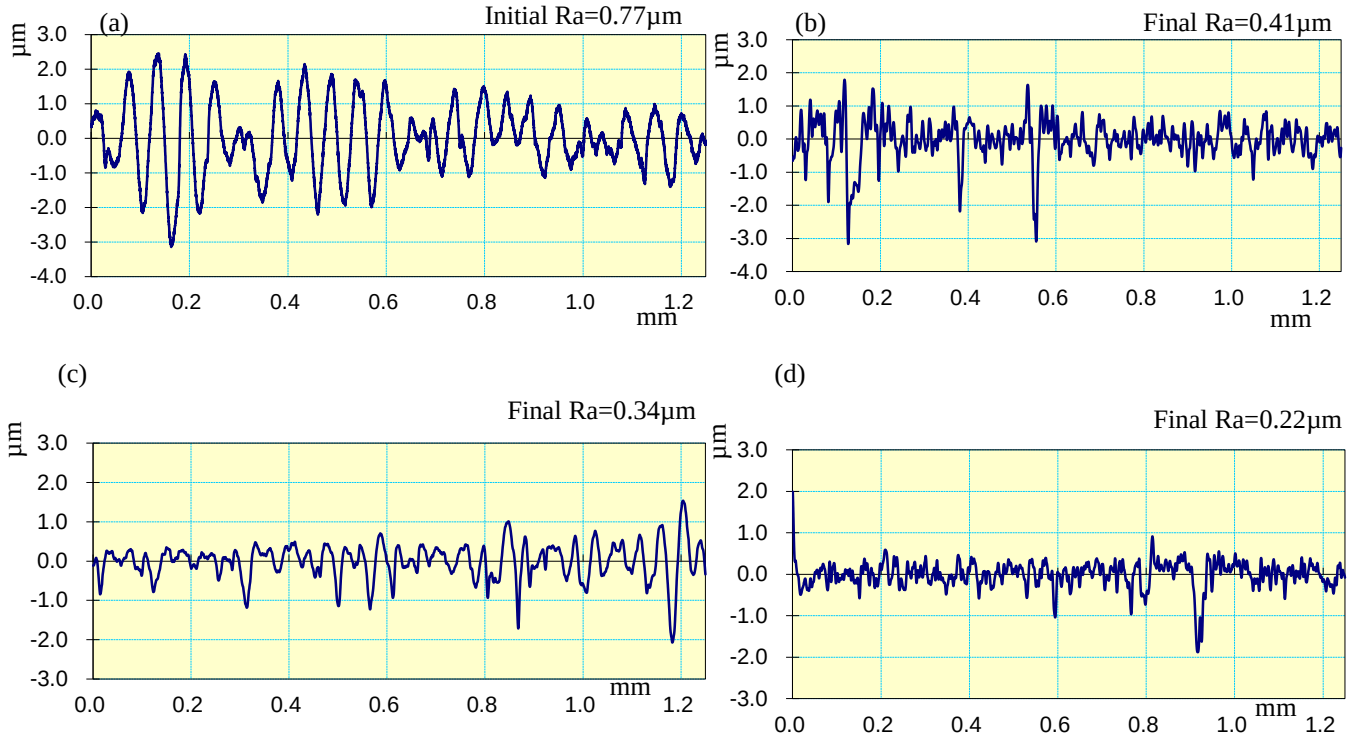

Figure 5.1: (a) Initial input measured profile, (b) after 200 cycle measured profile (c) measured final profile after 260 cycles (d) measured final profile after 320 cycle

For further microscopy study of initial and final finished surface, the scanning electron microscopy (SEM) analysis was carried out at 1500x magnification are shown in Fig. 5.1 (a) and (b), respectively. The initial surface after the internal surface grinding consists of various surface damages such as deeper grooves and cavity. After 780 numbers of finishing cycles, the micro-cutting takes place due to abrasion wear mechanism on the internal surface of ferromagnetic workpiece. The final finished surface morphology on the ferromagnetic workpiece surface due to the continuous reciprocation and rotational movement of active abrasive is shown in Fig 5.1 (b). The removal of surface damages after 780 numbers of finishing cycles which clearly results in better surface integrity on the internal surface of ferromagnetic. The overall results concluded that a significant improvement in surface quality was achieved during internal surface finishing of ferromagnetic workpiece with the present MR fluid based honing process.

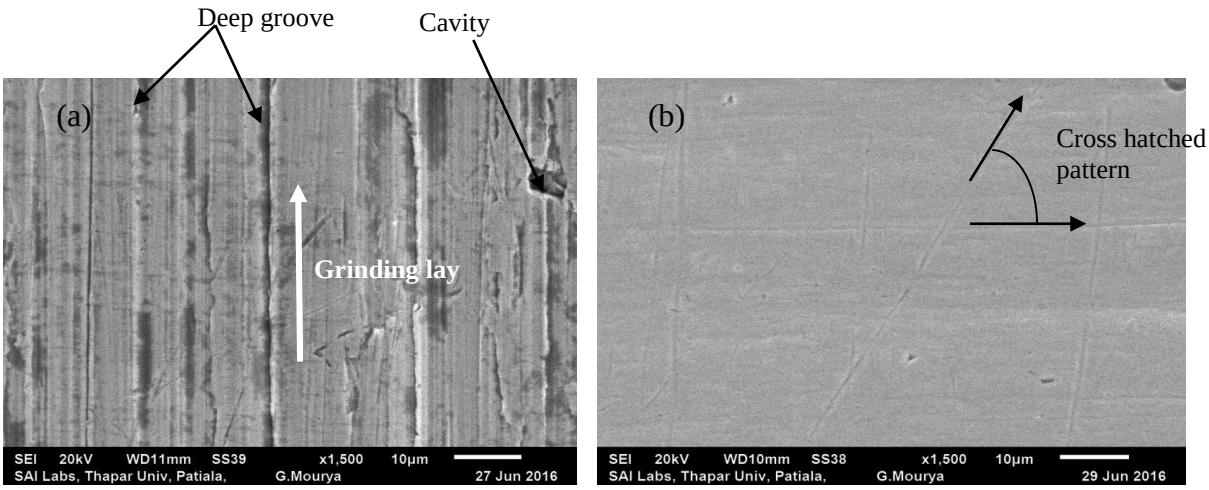

Figure 5.2: Surface morphology with Scanning electron microscopy of (a) initial ground surface (b) final finished surface after 320 finishing cycle at 1500x

Chapter 6 Conclusions

Mathematical model has been proposed for calculating the surface roughness of cylindrical workpiece through comprising parameters of the process. The model explores the effect of magnetic field density on the value surface roughness. To model the final surface roughness, modeling of magnetic field, magnetic force, and calculation for number of active abrasive particle, mass of a carbonyl iron particl (CIP), mass of susceptibility, are required. So modeling of magnetic field has done by using the Biot-Savart law for linear current and model of magnetic forece is available. Number of active abrasive particle and mass of CIP are calculated on the basis of MRP fluid material, and arrangement of workpiece and tool setup. A Matlab program has been made for calculation of magnetic filed density, by taking 1.5 ampere current, 750 numbers of turns, z from 0.015 m to 0.016 m with increament of 0.002 m. Mass of susceptibility is calculated from the available M-B curve of CIP CS grade material. Using all modeled and calculated parameters surafce roughness is calculated through MATLAB program made for calculation of surface roughness. Theoretically calculated surface roughness is validated with experimental surface roughness. While modeling and simulating the surface roughness in the magnetorheological (MR) honing process some important facts have been concluded which are as follows :

- Magnetic flux density decreases from 0.3738 T at finishing surface of tool core to 0.2939 T at the internal surface of ferromagnetic cylindrical workpiece following linear trend line with negative slope.
- As magnetic force is in direct relative with magnetic force therefore, the magnitude of force acting on SiC abrasive particle through CIPs decreases from 2.3937 X 10^{-10}N at finishing surface of tool core to 2.0107 X 10^{-10} N at workpiece surface.
- The size of SiC abrasive particle effects the quality of surface as depth of indentation and diameter of SiC grains are related with each other.
- In present study while validation of the model of surface roughness it was found that the roughness value obtained from theoretical calculation was 4.88% more than that of experimental measured roughness values which can be said that theoretical and experimental roughness values are in good agreement.
- From the scanning electron morphology (SEM) images, it was found that there was significant improvement in the surface quality due to abrasion wear on the internal

ferromagnetic cylindrical surface during finishing with the present MR fluid based honing tool.

References

[1] Sadiq, A. and Shunmugam M. S., (2010), A novel method to improve finish on non-magnetic surfaces in magnetorheological abrasive honing process, *Tribology International*, 43: 1122- 1126.

[2] Tani, Y. and Kawata K., (1984), Development of high-efficient fine finishing process using magnetic fluid, *Annals of the CIRP*, 33: 217-220.

[3] Kordonski W. and Jacobs S.D., (1996), Magnetorheological finishing, *International Journal of Modern Physics B*; 23–24(10): 2837–48.

[4] Singh, S. and Shan, H. S., (2002), Development of magneto abrasive flow machining process, *International Journal of Machine Tools* & *Manufacturing*, 42(6): 953-959.

[5] Jha, S. and Jain V. K., (2004), Design and development of the magnetorheological abrasive flow finishing (MRAFF) process, *International Journal of Machine Tools & Manufacture*, 44: 1019–1029.

[6] Jain, V.K., (2009), Magnetic field assisted abrasive based micro-/nano-finishing, *Journal of Materials Processing Technology*, 209: 6022-6038.

[7] John A. Schey, (2016), Introduction to manufacturing processes, New York: *Mc Graw Hill Book Company*, 2nd ed: pp.12-15.

[8] Jain, V.K., (2008), Abrasive-based nano-finishing techniques: an overview, *Machining Science and Technology*, 12(3): 257-294.

[9] Mori, Y., Yamauchi, K., Endo, K., (1987), Elastic emission machining, *Precision Engineering* 9(3): 123-128.

[10] Jha, S., Jain, V.K., (2006), Modeling and simulation of surface roughness in magnetorheological abrasive flow finishing (MRAFF) process, *Wear*, 261: 856-866.

[11] Umehara, N., Kirtane, T., Gerlick, R., Jain, V.K., Komanduri, R., (2005), A new apparatus for finishing large size large batch silicon nitride (Si3N4) balls for hybrid bearing applications by magnetic float polishing (MFP). *International Journal of Machine Tools and Manufacture*, 46: 151–169.

[12] Shinmura, T., (1987), Study on magnetic abrasive finishing - characteristics of finished surface. *Journal of Japan Society of Precision Engineering*, 53(11): 1791-1793.

[13] Singh, D.K., Jain, V.K., Raghuram, V., (2004), Parametric study of magnetic abrasive finishing process. *Journal of Materials Processing Technology*, 149: 22-29.

[14] Jayswal, S.C., Jain, V.K., Dixit, P.M., (2005), Modeling and simulation of magnetic abrasive finishing process, *International Journal Advanced Manufacturing Technology*, 26: 477–490.

[15] Singh, A.K., Jha, S., Pandey P.M., (2011), Design and development of nanofinishing process for 3D surfaces using ball end MR finishing tool, *International Journal of Machine Tools & Manufacture* 51: 142–151.

[16] Sadiq, A., Shunmugam M. S., (2010), A novel method to improve finish on non-magnetic surfaces in magnetorheological abrasive honing process, *Tribology International*, 43:1122- 1126.

[17] Tingzhang, W., Mingjun, C., Henan, L., Jiang, X., (2015), Development of a magnetorheological finishing machine for small-bore part of irregular shape and experimental study, *American Journal of Engineering and Applied Sciences*, 8 (3): 399-404.

[18] Jha, S. and Jain V. K., (2006), Modeling and simulation of surface roughness in magnetorheological abrasive flow finishing (MRAFF) process, *Wear*, 261: 856–866.

[19] Das, M., Jain, V. K., Ghoshdastidar, P. S., (2008), Fluid flow analysis of magnetorheological abrasive flow finishing (MRAFF) process, *International Journal of Machine Tools & Manufacture* 48: 415–42.

[20] Schinhaerl, M., Vogt, C., Geiss, A., Stamp, R., Sperber, P., Smith, L., Smith, G., Smith, R., (2008), Forces acting between polishing tool and workpiece surface in magnetorheological finishing, *Proc. of SPIE,* 7060 (706006): 1-12.

[21] Sidpara, A., Jain, V.K., (2011), Experimental investigations into forces during magnetorheological fluid based finishing process. *International Journal of Machine Tools and Manufacture*, 51: 358-362.

[22] Sidpara, A., Jain, V.K., (2012), Theoretical analysis of forces in magnetorheological fluid based finishing process. *International Journal of Material Sciences*, 56: 50-59.

[23] Singh, A.K., Jha, S., Pandey P.M., (2013), Mechanism of material removal in ball end magnetorheological finishing process, *Wear*, 302: 180-1191.

[24] Sidpara, A., Jain, V.K., (2013), Analysis of forces on the free form surface in magnetorheological fluid based finishing process. *International Journal of Machine Tools and Manufacture*, 69: 1-10.

[25] Kumar, S., Jain, V. K., Sidpara, A., (2015), Nanofinishing of freeform surfaces (knee joint implant) by rotational-magnetorheological abrasive flow finishing (R-MRAFF) process, *Precision Engineering*, http://dx.doi.org/10.1016/j.precisioneng.2015.04.014

[26] Wang, Y., Hu, D., (2005), Study on the inner surface finishing of tubing by magnetic abrasive finishing, *International Journal of Machine Tools and Manufacture* 45: 43-49.

[27] Sadiq, A., Shunmugam, M. S., (2009), Magnetic field analysis and roughness prediction in magnetorheological abrasive honing (MRAH), *Machining Science and Technology: An International Journal*, DOI: 10.1080/10910340903011805.

[28] Kang, J., George, A., Yamaguchi, H., (2012), High-speed internal finishing of capillary tubes by magnetic abrasive finishing, *Procedia CIRP*, 1: 414-418.

[29] Schmitt, C., Moos, U., Bahre, D., (2013), Comparison of different approaches to force controlled precision honing of bores, *Journal of Mechanics Engineering and Automation*, 3: 764-771.

[30] Judal, K.B., Yadava, V., Pathak, D., (2013), Experimental investigation of vibration assisted cylindrical magnet abrasive finishing of Aluminium workpiece, *Materials and Manufacturing Processes*, 28: 1196-1202.

[31] Yamaguchi, H., Shinmura, T., (2004), Internal finishing process for alumina ceramic components by a magnetic field assisted finishing process, *Precision Engineering* 28: 135–142.

[32] Jang, K. I., Nam, E., Lee, C. Y., Seok, J., Min, B. K., (2013), Mechanism of synergetic material removal by electrochemomechanical magnetorheological polishing, *International Journal of Machine Tools & Manufacture* 70: 88–92.

[33] Misakian, M., (2000), Equations for the magnetic field produced by one or more rectangular loops of wire in the same plane, *Journal of Research of the National Institute of Standards and Technology*, 105: 557-564.

[34] Niranjan, M. S., Jha, S., (2014), Flow behavior of bidisperse MR polishing fluid and ball end mr finishing, *Procedia Materials Science*, 6: 798 – 804.

[35] Pattanaik, L. N., Agarwal, H., (2014), Development of magnetorheological finishing (MRF) process for freeform surfaces, *International Journal of Advanced Mechanical Engineering*, 4: 611-618.

[36] Tricard, M., Korodonski, W. I., Shorey, A. B., (2006), Magnetorheological jet finishing of conformal, freeform and steep concave optics, *Annals of the CIRP Vol.* 55/1/2006

[37] Seok, J., Kim, Y.J., Jang, K.I., Min, B.K., Lee S. J., (2007), A study on the fabrication of curved surfaces using magnetorheological fluid finishing, *International Journal of Machine Tools & Manufacture*, 47: 2077– 2090.

[38] Sidpara, A., Das, M., Jain, V. K., (2009), Rheological characterization of magnetorheological finishing fluid, *Taylor & Francis*, DOI: 10.1080/10426910903367410.

[39] Gheisari, R., Ghasemi, A.A., Jafarkarimi, M., Mohtaram, S., (2014) Experimental studies on the ultraprecision finishing of cylindrical surfaces using magnetorheological finishing process, *Production & Manufacturing Research*, 2: 550-557.

[40] Jung, B., Jang, K. I., Lee, S. J., Seok, J., Min, B. K., (2009), Magnetorheological finishing process for hard materials using sintered iron-CNT compound abrasives, *International Journal of Machine Tools & Manufacture* 49: 407–418.

Appendix

(1) MATLAB Program to Calculate Magnetic Field in the Gap between Surface of Tool core Inner Surface of Cylindrical Workpiece.

```
clc
clear all
close all
x1=0;
y1=0;
a=2.7; b=12.7;
x=2.7; y=12.7;
z=0;
I=1.5;
if z<=15
    m=600*4*3.14*10^-7
else if z>16
        m=600*4*3.14*10^-7
    else
 m=605*4*3.14*10^-7
    end;
end;
n=700
pi=3.14;
i = 1;
for z1 = 15.155:0.001:16.155
r1=sqrt((x+x1)^2+(y+y1)^2+(z-z1)^2);
r2=sqrt((x-x1)^2+(y+y1)^2+(z-z1)^2);
r3=sqrt((x+x1)^2+(y-y1)^2+(z-z1)^2);
r4=sqrt((x-x1)^2+(y-y1)^2+(z-z1)^2);
r5=4*pi*((x+x1)^2+(z-z1)^2);
r6=4*pi*((x-x1)^2+(z-z1)^2);
r7=4*pi*((y+y1)^2+(z-z1)^2);
r8=4*pi*((y-y1)^2+(z-z1)^2);
Hx(i,:)=(I*(z-z1)/r5)*((b-y1)/r3+(b+y1)/r1)-(I*(z-z1)/r6)*((b+y1)/r2+(b-
y1)/r4);
Hy(i,:)=(I*(z-z1)/r8)*((a-x1)/r4+(a+x1)/r3)-(I*(z-z1)/r7)*((a+x1)/r1+(a-
x1)/r1);
Hz(i,:)=(I*(x+x1)/r5)*((b-y1)/r3+(b+y1)/r1)-(I*(y-y1)/r8)*((a-
x1)/r4+(a+x1)/r3)
+(I*(x-x1)/r6)*(-(b+y1)/r2-(b-y1)/r4)-(I*(y+y1)/r7)*((a+x1)/r1+(a-x1)/r2);
```

```
i = i+1;
end
Hxx = 10^3*Hx
Hyy=10^3*Hy
Hzz=Hz*10^3
Bx=m*Hxx*n
By=m*Hyy*n
Bz=m*Hzz*n
```

(2) MATLAB Program to Calculate Final Surface Roughness Values.

```
clc;
clear all;
close all;
format long
d=1.837235*10^(-6);%%%% d= depth of indentation corresponding on single SiC
particle

m=5320;          %%% m=number of active abrasive particle per stroke.
X=[Input the values of initial surface roughness data];
num_row = size(X,1);
num_col = size(X,2);
 Y=zeros(1,num_row);
f = d*m;
Y=X;
for j=1:1:25      %%% j is the number of finishing cycle
    for i=1:1:num_row
        if (Y(i))>=0
            Y(i)=X(i) -(f*j);
        else
                Y(i)=Y(i);
%         if(Y(i))<=0
%            Y(i)=X(i);
%         else
%            Y(i)=X(i) -(f*j);
        end
     end
end
        disp(Y)
```